# The *fumier* sequences of El Mirador cave: an approach to fire as a sociocultural practice and taphonomic agent

Aitor Burguet-Coca, Héctor del Valle, Isabel Expósito, Ángela Herrejón-Lagunilla, Erika Buitkute, Dan Cabanes, Isabel Cáceres, Ángel Carrancho and Juan José Villalaín

## Abstract

*Fumier* sequences play a primary role in the study of livestock management and the use of space in prehistoric pastoralist societies. These sequences are formed when dung accumulated in sheepfold caves and rock shelters is burnt, resulting in an overlapping of burnt and unburnt sedimentary layers. Thus, fire is a key taphonomic agent in the formation and alteration of *fumier* sequences.

The characteristics, functions, and management of burning events influence the preservation of the macro- and micro-remains potentially biasing the

A. Burguet-Coca(*), H. del Valle, I. Expósito, E. Buitkute, I. Cáceres

Institut Català de Paleoecologia Humana i Evolució Social (IPHES-CERCA), Zona Educacional 4, Campus Sescelades URV (Edifici W3), 43007
Tarragona, Spain

Universitat Rovira i Virgili, Departament d'Història i Història de l'Art, Avinguda de Catalunya 35, 43002
Tarragona, Spain

e-mail: aitorburguetcoca@gmail.com; hectorvalleblanco@gmail.com; iexposito@iphes.cat; erika.buitkute@gmail.com; icaceres@iphes.cat

Á. Herrejón Lagunilla
Departamento de Física, Universidad de Burgos,
Burgos, Spain.
Departamento de Física de la Tierra y Astrofísica. Plaza Ciencias 1. 28040. Facultad de Ciencias Físicas. Universidad Complutense de Madrid
Madrid. Spain
E-mail: angelaherrejonlagunilla@gmail.com; aherrejon@ubu.es; anherrej@ucm.es

J. J. Villalaín
Departamento de Física, Universidad de Burgos,
Burgos, Spain.
E-mail: villa@ubu.es

D. Cabanes
Department of Anthropology, Rutgers University, Biological Sciences Building, 32 Bishop Street, New Brunswick, New Jersey, USA.
e-mail: dan.cabanes@rutgers.edu

Á. Carrancho
Área de Prehistoria, Departamento de Historia, Geografía y Comunicación, Universidad de Burgos
Burgos, Spain.
e-mail:

*Corresponding author: Aitor Burguet-Coca e-mail: aitorburguetcoca@gmail.com

interpretation of the archaeological record. Therefore, it is important to understand the taphonomic effects of fire in *fumier* sequences.

In this chapter, we use a multi-scalar and interdisciplinary approach to the study of burning events at El Mirador cave. We analyzed the phytolith, fecal spherulites, pollen, non-pollen palynomorphs (NPP), and parasite remains in the *fumier* sequence, together with the mineral (FTIR) and magnetic properties of the sediments. In addition, we studied the effects of fire on the macrofaunal assemblages. The results obtained here provide the basis for a tapho-diagenetic framework that illustrates robustly the formation dynamics of the El Mirador *fumier* sequences.

## 1 Introduction

Fire is a structural agent in the formation of a type of archaeological sequence called a *fumier*, a French term used to describe sedimentary sequences produced by the accumulation and burning of dung in prehistoric caves and rock shelters. The deposit of El Mirador cave mainly constitutes a *fumier* sequence, which contains an extensive and varied archaeological record. Since Brochier first described this type of sequence from a geoarchaeological and geo-ethnoarchaeological perspective (Brochier, 1991, 1983; Brochier et al., 1992), the phenomenon of sheepfold caves has been documented throughout the Mediterranean basin (Angelucci et al., 2009). The earliest studies of *fumiers* focused on describing these sequences at a macro- and microscopic scale in order to identify them in archaeological sites (Angelucci et al., 2009; Canti, 1999; Macphail et al., 1997; Shahack-Gross, 2011). Macroscopically, *fumier* sequences have been described as complex stratigraphies made up of anthropogenic sediments resulting from the accumulation of burned and unburned dung, generating successive thin sub-horizontal layers that exhibit abrupt terminations and constant lateral changes (Brochier et al., 1992; Friesem, 2016; Goldberg and Macphail, 2006; Macphail et al., 1997). The term *facies* at El Mirador cave, make reference to archaeo-sedimentary units based on chromatic, texturing and composition variations (for facies description see Angelucci et al., 2009; Vergès et al., 2016a). *Facies* have been related to the conditions and characteristics of combustion, as well as to the humidity,

compaction or degradation conditions of the dung before burning (Angelucci et al., 2009; Vergès, 2011; Vergès et al., 2016b). A scarcity of archaeological material has also been proposed as a characteristic trait of *fumier* sequences (Angelucci et al., 2009), although in the specific case of El Mirador cave this criterion is not met, as an abundant and varied archaeological record has been documented throughout the sequence (Vergès et al., 2016a). Microscopically, *fumier* sequences have been characterized by the identification of microlaminations, dung spherulites, authigenic phosphates and abundant phytoliths (Canti and Brochier, 2017; Shahack-Gross, 2011; Shahack-Gross et al., 2005, 2003).

The macro- and microscopic records that characterize *fumier* sequences are affected by the use of fire for economic and cultural purposes, linked to the reduction of the volume of accumulated dung (Acovitsioti-hameau et al., 1999; Macphail et al., 1997; Shahack-Gross et al., 2005; Vergès et al., 2016b) and the cleaning of penning space (Acovitsioti-hameau et al., 1999; Brochier, 2005, 1991). Although these practices have been extensively identified in the Mediterranean archaeological record, their impact on the formation and preservation of the archaeological record has not been addressed yet.

In this chapter we present a multidisciplinary approach to fire as a taphonomic agent, determining burning conditions and its incidence in macro- and microscopic assemblages. To do this, we performed a multidisciplinary analysis based on a wide range of studies and to describe the effects of combustion generated by the burning of dung, in order to subsequently examine the formation processes. Understanding the role of fire in the formation, alteration, and destruction of the archaeological record is necessary to correctly interpret the archaeological record, both at El Mirador cave and in other archaeological sites containing *fumier* sequences. Here we include the results from archaeomagnetism, palynology, paleoparasitology, FTIR (applied to sediments and bones), phytolith analyses, and bone diagenesis analysis. The structure of the chapter is around two main objectives: First, to evaluate the impact of fire in the preservation of the macro- and micro-archaeological record contained in *fumier* sequences. Second, to understand and characterize the combustion of dung and its importance as a livestock management practice.

The materials studied in this chapter come from different areas and levels of El Mirador cave and the methods used encompass different fields of study and approaches. For this reason, we have summarized the materials included in this chapter in Supplementary information 1 and the description of the methods in Supplementary Information 2.

## 2 Results

### 2.1 Bone diagenesis

From a microscopic perspective, El Mirador cave raises questions about the preservation of bone remains. Bone diagenesis refers to physical and chemical degradation of bone materials over time. Monitoring diagenetic parameters is important in order to achieve high enough resolution to obtain biomolecular information, but it is also important in order to understand cultural and taphonomic processes. This is the case of boiled, cooked, and intentionally burned bones or bones non-intentionally burned during *fumier* formation.

The bone assemblage from four facies (*a*, *v*, *tf*, *r(m)*) has been analyzed (Supplementary Information 1) focused on bone preservation and taphonomic features that allow distinguishing between *facies* (Del Valle et al., 2022).

In facies *a*, the bone collagen and bioapatite crystals are well preserved, with crystallinity index (CI) values around 3.59 ±0.55 (Supplementary Information 3). Crystallinity values also are strongly related to the carbonate / phosphate ratio (C/P), suggesting incorporation of carbonate ions ($CO_3^{2-}$) in the crystal lattice. However, this absorption does not translate into the incorporation of calcium carbonate. These data suggest that the bone of facies *a* preserve a high collagen amount, slightly high C/P, and low CI in no burned bones remains (Supplementary Information 3).

As for facies *v*, the unaltered and boiled bones have retained good percentages of collagen content, even recovering 16% of extracted collagen (18% concerning 3.60 N wt% through estimated collagen by ATR-FTIR) (Supplementary Information 3). The crystallinity index is consistent with the results of the collagen content, with an CI of close to 3.45±0.09. In other words,

the crystalline lattice is preserved in stable degrees because a sufficient fraction of collagen content is preserved (Hedges, 2002). These values are close to the modern bone values and, therefore these bones are considered to be well-preserved (WP). However, the need to evaluate the bone remains individually before being used for isotopic analyses is pointed out due to the slight increase in $CO_3^{2-}$ ions observed, especially for boiled bones (C/P= 0.33±0.03). In this type of facies is identify boiled bones, however, this taphonomic modification in the *fumier* deposits needs to be further investigated (Supplementary Information 3). Boiled bones are identifiable at the macroscopic level in keeping with the criteria proposed by several authors (Nicholson, 1996, 1998; Botella, 2000; Martín-Rodriguez, 2016). It is said, smoothness, light transparency, yellowish-cream color, and oily bone surface (White, 1992; Botella et al. 2000; Pijoan et al., 2007; Cáceres et al., 2007). In our results, boiled remains have presented a good amount of preserved collagen confirming what has already been reported in other studies (Roberts et al., 2002; Koon et al., 2003, 2010: Munro et al., 2007), even recording Amide III (Chadefaux et al., 2009; Bobbroff et al., 2016; Leskovar et al., 2020).

It was observed that in the diagenetic parameters of facies *a* and *v* statistically significant differences are not observed except for the API index, that is, a difference from A-type carbonates in the crystal lattice of bioapatite. This is important because it has been suggested that A-type carbonate substitution could be given when water is excluded from the burial environment (Bayarı et al., 2020), affecting bone preservation in facies *a* (Del Valle et al., *2022*).

In facies *tf*, the preservation of the collagen content in the bones is very homogeneous and close to 3%, which means recrystallization occurred, increasing the CI values around 4.06±0.29 (Supplementary Information 3). In other words, the bones underwent a thermal impact close to carbonization at 300 ºC in a more or less homogeneous way (Fig. 1a). These results are interpreted as postdepositional burning and cleaning. The reduced carbonate content is according to this thermal alteration as it has been observed in other experimental works (Lebon et al., 2010, Marques et al., 2018). The bones of the facies *tf* are characterized by a high crystallinity index and reduced carbonate and organic content values.

**Fig. 1 a.** Example of ATR-FTIR spectra of bone samples from facies and assignments of the main bands. **b.** Sediment spectra of some of the studied samples. MIR104-187 facies *b*; MIR104-103 facies *c*; MIR105-106 facies *a*; MIR105-101 facies *a*

Facies *r(m)* has been characterized as a light brown massive accumulation of ash. The CI obtained in the bone remains is around 5.39 ±0.39 with the complete degradation of collagen (Supplementary Information 3). Studying the exposure of the bones to high temperatures through the use of ATR-FTIR and bone surface show that they reached temperatures in the range close to 700 ºC (Fig. 1a). The carbonate content is very low due to the significant loss of the bioapatite carbonate content during cremation. Secondary calcite was observed related to the sediment composition (mainly ash).

For the sediment, it is a benign and non-corrosive soil for the conservation of bones with a pH =~8 (Karkanas et al., 2000; Weiner, 2010). It is characterized by loamy substrate with moderately alkaline pH values, high $Ca^{2+}$, and, in general, have higher organic contents than corrosive soils. All facies are characterized by maintaining a basic pH. Starting from the Mas del Pepet experimental context (del Valle, 2018; Vergès et al., 2016b), it is seen that the ash burned sediments have high basicity after burning (pH=~13), which is buffered over time to values close to pH = ~8 due to $CaCO_3$ amount, being observed in the burned facies of El Mirador cave (Del Valle, 2018).

## 2.2 FTIR from bulk sample

The facies analyzed by means of FTIR present variations in their mineralogical composition related to their differing formation processes. Facies *a*, *tf* and *v* of El Mirador cave are made up primarily of clay, followed by calcite, whereas in facies *b* and *r(m)* calcite dominates (Supplementary Information 4 and Fig. 1b). The presence of other minerals such as quartz, dahllite and opal is common in the composition of most of the samples.

In all of the facies studied, the calcite is pyrogenic in origin (ash) and is associated with thermally altered clay (Supplementary Information 4 and Fig. 1b). The exceptions are facies *a*, in which non-thermally altered clay was documented in some samples, and facies *v*, in which non-thermally altered clay and calcite of geogenic origin was found in a large number of samples.

The temperature reached during the combustion of dung in the El Mirador cave sequence can be determined using the identification of high disorder calcite (HDC) and the thermal alteration of the clay, which can be observed into account the positions of the major clay peaks on the spectra (Supplementary Information 4 and Fig. 1b). The combination of these two approaches to inferring paleotemperatures of the *fumier* record using FTIR indicates the presence of clear variations between the studied facies.

Facies *b* and specialty facies *r(m)*, reached temperatures of up to 600 ºC and facies *tf* temperatures are in all samples lower than 600 ºC. However, some samples from facies *b, r(m)* and *tf* containing HDC, indicative of having reached 800 ºC. On the other hand, the analysis of facies *c* suggests that its temperature never exceeded 600 ºC and the study of facies *v* identifies it as a present-day clay facies with no thermal alterations except for two samples, which evidence exposure to low temperatures (Supplementary Information 4). Only facies *a* exhibits significant internal variability, with samples containing calcite formed at high temperatures (>600 ºC), other samples with clay burned at low temperatures (400 and 500 ºC) and several samples without any thermally altered clay.

### 2.3 Rock magnetism

#### Reversibility of thermomagnetic curves

Magnetite or partially maghemitized magnetite (oxidized magnetite) was the main ferromagnetic mineral detected in the ash and subjacent carbonaceous facies (see Herrejón-Lagunilla et al., this book for further details). However, the degree of reversibility (coincidence between heating and cooling cycles) of the thermomagnetic curves is clearly different depending on the facies. The ashes tend to present highly reversible curves, indicating high thermomagnetic stability (Fig. 1b-e in Herrejón-Lagunilla et al., this book). This stability suggests that these facies may have reached temperatures of >700 ºC (the maximum temperature applied during the experiment). Otherwise, chemical changes due to heating would be expected.

Carbonaceous facies (facies c), on the other hand, systematically exhibit irreversible curves (Fig. 1f-g in Herrejón-Lagunilla et al., this book). The increase in magnetization on the cooling cycles is interpreted as the formation of secondary magnetite. The thermal instability is presumably caused by the relatively low temperatures (at least lower than 700 ºC) reached by these facies. The identification of partial thermoremanences in the carbonaceous facies with maximum unblocking temperatures up to 450 ºC (Herrejón-Lagunilla et al., this book) indicates that the maximum heating temperatures reached by this facies fall in that range. This has been previously observed at El Mirador site and elsewhere (e.g., Carrancho et al., 2009, 2013) and is in agreement with the lack of thermomagnetic reversivility observed in this facies. If it had been exposed to temperatures higher than those reached during the experiment (700 ºC), the sample would have been thermochemically stabilized and, consequently, no mineralogical transformation would have been observed during the experiment

**Fig. 2** Results of anisotropy of magnetic susceptibility (AMS) for the burning events Ci2 and Ci3 (level MIR 104), Ci5, Ci6 and Ci7 (level MIR107), ordered according to their relative stratigraphic position (Ci2 is the shallowest, and Ci7 the deepest). All of them were located in Sector 100. The graphics correspond to Equal area projection of the magnetic ellipsoid axes (left), corrected anisotropy degree [PJ] vs. magnetic susceptibility [Km] plot (center) and shape parameter [T] vs. PJ plot (right). In the equal area projection plot, K1 = blue squares, K2 = green triangles and K3 = pink circles (small symbols show the results for each specimen, and large symbols represent the mean direction). Confidence ellipses (95%) are also shown

## Anisotropy of magnetic susceptibility (AMS)

The corrected degree of anisotropy ($P_J$; Jelinek, 1981) was found to be low in all episodes (≤1.016) and magnetic foliation (oblate shape) predominates over magnetic lineation (prolate shape) (Table 1). Three main types of magnetic fabric were observed: (1) episodes with K1 (maximum axis), K2 (intermediate axis) and poorly defined K3 orientations (minimum axis) (Ci2 and Ci3, Fig. 3a-b); (2) episodes with K3 aligned with the vertical and K1 and K2 in the horizontal plane, with not very well defined orientations (Ci5 and Ci6, Fig. 3c-d); (3) episodes with K3 slightly tilted in relation to the vertical plane, and well-differentiated K1-K2 defining a magnetic foliation plane with K1 aligned with the maximum slope of this foliation plane (Ci7, Fig. 3e).

**Table 1** Statistical parameters of the anisotropy of magnetic susceptibility (AMS) (N= number of samples considered for the calculations / N'= total number of measured samples/ St. D = Standard deviation / $K_m$= susceptibility

value / L= magnetic lineation / F= magnetic foliation / $P_J$= corrected anisotropy degree / T= shape parameter)

Considering the sedimentary characteristics of prehistoric combustion structures like those studied here (Mallol et al., 2017), the expected fabric should be similar to that from well-preserved, natural cave sediments. This means that K3 should be perpendicular to the plane of the depositional surface and K1-K2 should form a girdle in the bedding plane (Tarling and Hrouda, 1993 and references therein). The vertical K3 is interpreted as an effect of gravitational forces during the formation episodes and posterior covering by younger materials. Magnetic fabric Type 2 (Ci5 and Ci6, Fig. 2c-d) presents a similar pattern. In the case of Type 3 (Ci7, Fig. 2e), the slight deviation of K3 in relation to the horizontal plane may be an effect of formation on a slight slope (e.g., Bradák et al., 2020). The alignment of K1 with the maximum slope inside the foliation plane is consistent with this explanation.

The poorly defined orientation of all the axes of Type 1 reflects the random orientation of the ferromagnetic grains in episodes Ci2 and Ci3 (Fig.2a-b). This could be interpreted as an effect of a mechanical process. However, the mean archaeomagnetic directions of these combustion episodes are not widely scattered and exhibit directions consistent with normal polarity, as is expected for the time at which they were formed. In fact, it must be said that the quality of the directional record of all the studied episodes is generally high, regardless of the type of magnetic fabric (see Herrejón-Lagunilla et al., this book). This indicates the relatively good preservation of the sample areas of these combustion episodes.

**White ash-like facies**

Finally, it is worth mentioning the particular behavior of white facies (described as type b) with an ash-like appearance taken from Ci2. Hysteresis cycles show a high contribution of the diamagnetic fraction and low content of ferromagnetic minerals (Fig. 3a). This explains the noisy thermomagnetic curves (Fig. 3b). Considering that ash facies presents high ferromagnetic (s.l.) mineral content (e.g., Carrancho et al., 2009; McClean and Kean, 1993; Peters et al., 2001), the evidence reported here strongly suggests that the white facies studied from the

Ci2 event is not actually an ash facies (s.s.) or, at least, its ash content is rather low. This anomalous behavior seems to be related to the identification of speleothem fragments in this facies observed in thin section analyses (Dr. A. Polo-Díaz, personal communication). As speleothems are extremely poor in ferromagnetic minerals, it would explain the low magnetic signal detected.

**Fig. 3 a-b**. Hysteresis loops and c-d. thermomagnetic curves (temperature vs. magnetization) of white facies from Ci2 event (level MIR104). Pannel e. shows the white patch inside Ci2.

### 2.4 Phytolith and fecal spherulite results

The phytolith results show a clear predominance of monocotyledons, classified as Poaceae (grasses) due to the absence of Cyperaceae and palm tree morphologies in the studied assemblages (Supplementary Information 5). The percentage of Poaceae is up to 90% in some samples from level MIR104. Most of the samples exhibit values between 80% and 90%, with one outlier in sample 188 from MIR104 (51.74%). Between 20 and 30% of grass morphotypes were determined as leaves/stem (ELONGATE ENTIRE and CYLINDROID ENTIRE), with only a few samples exceeding 30%. The morphotypes of grass inflorescences (Elongate dentate and Papillate) do not represent more than 10% of the phytolith assemblage.

The group of dicotyledonous plants (Blocky and Tabular entire) is represented with values below 10% of the total of the assemblage, except for sample 186 from MIR105 (15.15%). Anatomically, the identified morphologies related to wood and the values obtained for dicot leaves are irrelevant throughout the sequence.

Taphonomically, the most common alterations identified in the phytolith assemblages are weathered morphologies, and to a lesser extent, melted morphologies, although weathered morphotype never exceed 10% (Supplementary Information 5). The exceptions are the samples taken from the top of each level: in sample 108 from MIR105 13% of the morphologies were altered beyond recognition, and in sample 188 from MIR104 a total of 24% of phytoliths were weathered morphotypes. Most of the samples present a low percentage of phytoliths in anatomical connections, fewer than 10%, with

multicellular structures formed between two and three phytoliths per multicellular structure.

Fecal spherulite concentrations are in most cases much higher than the phytolith concentrations per unit of weight. Three samples have faucal spherulites concentrations exceeding 1000 million of phytoliths per gram of sediment, four samples have values of between 600 and 800 million, and the remaining samples were found to have values of between 50 and 600 million of faucal spherulites per gram of sediment (Supplementary Information 5). Yet, in most of the samples, the phytolith concentration is less than 250 million per gram of Acid Insoluble Fraction (AIF), and only four samples present values between 700 million and 1000 million. Sample 100 from level MIR105, is an exception in the sequence with a concentration of 1700 million phytoliths per gram of AIF.

The greatest variability on concentration results was documented in the phytoliths and spherulites, and several discontinuities were recorded within the sequence (Supplementary Information 5). Sample 188 from level MIR104 exhibited very low phytolith concentrations, with over 50% of the sample being the weathered morphotype. In the remainder of the samples, lower phytolith concentrations in facies *c* were lower than in facies *b*. In level MIR105, the highest concentrations, both for spherulites and phytoliths, were identified at the top and the base of the level, while a clear decrease in phytolith concentrations was recorded in the middle section.

### 2.5 Pollen results

The palynological analysis of the samples from level MIR4, which focused on the characterization of four sedimentary facies (*a*, *b*, *g*, *m)*, allowed for the identification of several general features. Samples from facies *a*, which has been described as yellowish-brown clayey silt with dispersed organic matter, ash and microcharcoal fragments, and facies *b*, *g* and *m*, which correspond to ashy layers related to different degrees of thermal disturbance. In addition to considering the pollen richness and taxonomic variability of pollen and non-pollen palynomorphs, we categorized the post-depositional damage observed in

the pollen grains into three types: thermal alteration, fragmentation and compaction (Expósito and Burjachs, 2016).

Fragmentation or thermal alteration grains are common and represent more than 20% of the remains identified. The maximum percentages of fragmentation (18.2%) were documented in samples from facies *g*, and the highest values of thermal alteration (30.4%) were in samples from facies *m*.

In addition, thermal alteration is the most relevant modification associated with low palynological concentrations. However, we found that oxidation did not give rise to the artificial over-representation of a specific pollen taxon when the results of the samples affected by thermal alteration were compared with the taxa numbers in the level average.

The expected characteristics of burned facies are a low CP, the presence of thermally altered pollen grains, little palynological taxonomic variability and low resolution for landscape reconstruction. In this sense, samples from same facies show similar results, mainly in terms of the preservation of the pollen record. However, we have observed that some of the facies classified as burned facies (especially *b* and *g*) include the input of pollen without burning damage.

### 2.6 Paleoparasitology results

All analyzed samples (Supplementary Information 1) contained micro-charcoals as well as other recognized particles, including phytoliths, spores, and pollen. All 20 samples were determined to be free of parasitological remains, although there were also five undeterminable microfossils (samples no. 1 and 44).

All of the undeterminable microfossils from El Mirador cave have some characteristics of potential parasite eggshells. Due to the lack of a complete set of current characteristics, scarce data, and endless other potential identification possibilities, we were unable to determine the nature of these specimens.

## 3 Discussion

### 3.1 Fire as a taphonomic agent: the alteration of micro and macroscopic assemblages in *fumier* sequences

To sum up, as a taphonomic agent, fire, influences the preservation of the archaeological record in the aftermath of *fumiers* in a variety of ways. Phytoliths and spherulites resist the effects of fire well because of their mineral composition and concentration process generated by fire. On the other hand, other micro-remains such as parasites and pollen tend can be altered or even obliterated by the action of fire at high temperatures. However, the preservation of pollen grains can be quite good if they are deposited after burning. This differential pattern in deposition and preservation may explain the abundance of phytoliths and spherulites, and in some cases pollen, in *fumier* sequences, and why they have been identified as a defining feature of this type of archaeological sequence (Angelucci et al., 2009; Shahack-Gross, 2011). The faunal assemblages, like the micro-remain assemblages, present different diagenetic trajectories that influence the macroscopic preservation of the assemblage as well as its mineral composition.

The presence of micro-remains, especially phytoliths and spherulites, and autogenic minerals like carbonate hydroxylapatite (dahllite) or calcite of pyrogenic origin is one of the most diagnostic traits of *fumier* sequences (Angelucci et al., 2009; Shahack-Gross, 2011). These micro-remains preserved in dung pellets provide key information about aspects related to diet, herd composition, seasonality, environment and landscape characteristics, enclosure spaces, and cave use, among others (Albert et al., 2008; Burguet-Coca et al., 2020; Delhon et al., 2008; Panadès et al., 2016; Portillo and Albert, 2011). The high temperatures identified in dung combustion have not completely eliminated these diagnostic micro-residues, demonstrating their resistance to the action of fire (Burguet-Coca et al. 2020; Portillo and Albert, 2011). Phytolith alterations are generally low and mainly weathered-type chemical alterations, with a low presence of melted morphologies indicative of fire alteration. The resistance of phytoliths at these temperatures is explained by their silica composition, which has a melting point of 1,713 ºC (Piperno, 2006). Furthermore, sedimentary contexts formed by large amounts of organic matter and urine can lower the melting point of phytoliths to between 600 ºC and 900 ºC (Matthews, 2010;

Brönnimann et al., 2017; Canti and Brochier, 2017). Apparently, the phytolith assemblages at El Mirador are not particularly affected by fire. The uppermost samples from the MIR104 and MIR105 units show phytolith weathering associated with subaerial exposure and dissolution by water. In addition, these phytolith assemblages were previously affected by fire.

Dung spherulites survive at temperatures below 650–700 ºC (Canti, 1999; Matthews, 2010; Shahack-Gross, 2011). Although temperatures higher than those exceeding this threshold have been documented by FTIR and Rock-magnetism in the sequences studied, it seems that they did not completely affect the spherulite assemblages. The large number of spherulites produced by herbivores such as goats or sheep increases their preservation chances despite fire effects. Furthermore, volume reduction processes together with variable temperatures within the same heap can favor the concentration and, as a result, the preservation of spherulites, giving rise to variable quantities identified in the El Mirador sequence.

However, fire has generated a process of concentration that may have relevance in the interpretation of both the macro- and microscopic record. This process is related to the reduction of the volume in which botanical remains such as phytoliths and mineral remains such as spherulites are concentrated and can also generate concentrations of archaeological remains such as bones, lithic industry and ceramics. Some experimental have found that burning can reduce the initial volume of accumulated material by 80 to 90% (Shahack-Gross et al., 2005; Vergès et al., 2016). In short, the material accumulated in one meter of dung is concentrated in 10 to 20 centimeters after burning. In addition, the new entry of animals into the cave or pressure from the sediments themselves can generate even finer facies where the macroscopic archaeological material will concentrate further. Volume reduction and materials concentrations may increase the challenges for interpreting the archaeological record on a spatial-temporal scale. Even so, the analysis of anisotropy of magnetic susceptibility and paleomagnetic results (Herrejón-Lagunilla et al., this book) show good preservation of the archaeomagnetic directions in the studied facies. It is worth to mention that, in a strict sense, archaeomagnetic directions are recorded after the heating, during the cooling (just when the blocking

temperature is surpassed). That is, this process takes place when the greatest volume reduction has already occurred.

The lack of parasite remains can be attributed to the effectivity of burning practices to eliminate them and prevent the spread of potential infections. This is likely the result of the burning practices that took place in the cave, which pays testimony to the effectiveness of burning strategies for cave cleaning and disease prevention purposes. Indeed, the practice seems to have exterminated any existing parasites, thereby preventing the spread of potential infections (Acovitsioti-hameau et al., 1999; Brochier, 2005). However, it is not possible to rule out that biotic decomposition or abiotic processes could also have led to the absence of parasites, especially in facies apparently without apparent fire impact.

Pollen grains undergo specific alteration processes that are different from other micro-remains present in *fumiers* such as phytoliths, spherulites or parasites. The differential preservation of pollen grains in archaeological deposits is commonplace and expected. Several taphonomic works have explored the representativeness and reliability of palynomorph assemblages from archaeological sites in caves (Weinstein-Evron, 1981; Weinstein-Evron, 1994; Coles et al., 1989; Diot, 1991; Simpson and Hunt, 2009). Processes such as burning, recycling and bioturbation can relocate material throughout archaeological deposits and soils and can produce marked biases in the pollen record (Bryant et al., 1994; Bryant and Holloway, 1996). Specifically, fire contributes to the alteration of pollen assemblages, as high temperatures can affect their preservation and generate observable morphological features.

However, in the burned facies at El Mirador cave (especially *b* and *g*), the pollen does not always reflect the alterations typical of the processes that the sediment at the site has undergone. This could imply that pollens without thermal alterations were deposited on the burned facies after the combustion event. These assemblages represent an important contribution to our understanding of the modification of the landscape and human pressure on plant environments.

The use of fire in *fumier* sequences modifies bone remains in several ways. The practice may reflect a mixture of anthropic processes related to the mastery of fire. However, distinguishing between these different possible anthropogenic processes (i.e., intentional burning, cooking, boiling, roasting, hearths, etc.) can prove challenging. This issue also arises when examining and attempting to classify boiled, cooked and intentionally burned bones from bones burned non-intentionally during the formation of the *fumier* (Del Valle, 2018).

One of the main aims of the analysis of burned bones is to detect those exposed to low temperatures affecting bones and cooking processes in order to better understand the cooking activities of past peoples. However, due to the burning processes that characterize *fumier* sequences, it was only possible to identify these cooked faunal remains in the unburned facies (facies *v*). However, to optimize the identification of such remains, the diagenetic modifications that can occur must also be considered.

The preservation of bones in *fumier* contexts is good once a neutral pH environment is reached. As Nicholson (1996, 1998) described in reference to compost heap experiments, burned bones tend to be well-preserved as a consequence of the cross-linking of collagen with humic substances in the soil (neutral pH reached), resulting in a structure resistant to enzymatic attack. The preservation of bones in *fumier* sequences presents two clean trends. First, the diagenetic pathway of the unburned facies *v* and bones unburnt in re-elaborated facies *a*, which implies good preservation of organic material with a differential but low thermal impact. Second, the pathway of the burned facies *tf* and *r(m)*, in turn, illustrate two trends based on the temperatures reached: the accelerated hydrolysis of collagen and the loss of previous biostratinomic processes due to cremation.

### 3.2 The role of fire: management of sheepfold caves and characteristics of dung combustion

At the El Mirador cave, the characteristics of the combustion of dung, especially the paleotemperature, have been approached through the mineralogical analysis of sediments and bones by means of FTIR and rock magnetic analysis.

Additionally, the complete absence of parasites remains and the low presence of pollen grains in some facies also has been used as an indirect paleotemperature reference. For the ashy facies, the results are consistent in determining high combustion temperatures for facies *r(m)* and *b* and lower for facies *tf* (<600 ºC). The results for facies *c* (carbonaceous) point to a lower temperature, with results yielding more variable definitions depending on the analysis technique used, but coinciding with a carbonization process such as that which characterizes this facies (Angelucci et al., 2009). As far as the magnetic analyses are concerned, the carbonaceous facies reached maximum heating temperatures of around 450 – 500 ºC. These ashes and carbonaceous facies correspond to the remains of the combustion episode and the basis of the combustion episode, respectively (the floor above which the fire was done and that resulted thermally altered) and have been identified in other *fumier* sequences (Polo-Díaz et al., 2014, 2016; Égüez et al., 2016), and were observed in the Mas del Pepet experimental project as well (Vergès et al., 2016).

The results of the FTIR of the sediments and faunal remains are also consistent when characterizing facies *a* as that with the most internal variability in terms of temperatures reached by both the sediments and the bones. In this case, the divergent presence of fire is related to removal processes that generated facies with multiple origins. This observation based on the analysis of the archaeological record from the facies at the site supports the proposal to define these facies *a* using a micromorphological approach (Angelucci et al., 2009).

The temperatures identified in burned episode identified in level MIR105 are consistent with those of experimental works that replicate the combustion of dung (Vergès, 2011; Martín-Rodríguez and Vergès, 2016; Vergès et al., 2016; Burguet-Coca and Expósito, 2018). However, these experimental references document differences in temperature within the same heap. In the archaeological sequence, although dung piling is the most likely formation method, it has not been possible to specifically study the differences in temperature within the same heap. The experimental references focus on the documentation of the temperatures in the ash facies, and do not provide data on the formation of carbonaceous facies such as facies *c* identified in the El

Mirador cave deposit. Facies c (carbonous facies) developed below the facies b (ash facies), with different conditions and lower temperatures (Burguet-Coca, 2020; Vergès et al., 2016b). In addition, the temperatures that are reached in a *fumier* sequence are related to the condition of the dung before combustion, which includes variables such as compaction, disintegration, humidity, degradation and the period of the year in which the cave was occupied before the combustion (Vergès, 2011; Vergès et al., 2016; Burguet-Coca and Expósito, 2018). With the high temperatures identified in Sector 100 of El Mirador cave through FTIR and rock magnetic analysis, it is quite possible that the burned dung had good characteristics for combustion in terms of humidity and degradation.

## 4 Conclusion

In this multidisciplinary approach to the El Mirador cave sequences, we have been able to observe different patterns of alteration and preservation of the macro- and micro-archaeological assemblages. The impact of fire varied depending on the material it affected. We characterized fire as the primary agent of alteration in the different facies studied and found evidence that the ash facies reached high temperatures (> 600–700 ºC), as opposed to the lower temperatures (up to 450–500 ºC) reached by the subjacent carbonous facies. Not only fire alter archaeological remains and micro-remains, it can also significantly reduce the volume of accumulated material, resulting in concentration phenomena with considerable implications for the evaluation of the diachrony of the levels and their socioeconomic significance. In this chapter, we have attempted an initial analytical effort to link combustion with the preservation of the archaeological record from a multiscale perspective in order to do a better interpret prehistoric *fumier* sequences. Recognizing and evaluating these alteration processes has proven one of the greatest challenges to extracting the most information possible from the *fumier* sequence at El Mirador cave with regard to livestock activities, stabling spaces and the management of livestock landscapes, among many other aspects. Assessing the impact of fire – the primary agent of alteration – on this type of archaeological sites is the key to correctly interpreting the archaeological record. Known the important effects of the fire in archaeological deposits,

assessing its impact on these records is essential to understand their formation and alteration. Thus, it is necessary to face this assessment when starting any work in a deposit like prehistoric sheepfold caves.

**Acknowledgments**

Authors thank the support of the Spanish Ministry of Universities and European Union-NextGenerationEU (Margarita Salas Grants), European Social Fund (Operational Programme for Castilla y León) and the Junta de Castilla y León (Consejería de Educación). The support of the projects PID2019-107113RB-I00 / AEI / 10.13039/501100011033, PID2019-105796GB-I00 / AEI / 10.13039/501100011033 and PID2019-108753GB-C21/ AEI / 10.13039/501100011033 (financed by Agencia Estatal de Investigación, Spain) and BU235P18 (funded by Junta de Castilla y León and European Fund of Regional Development) is also appreciated by the authors. This research was developed within the framework of various projects from the Spanish Government-MICINN-FEDER (PGC2018-093925-B-C32) and Generalitat de Catalunya-AGAUR projects (2017 SGR 836 and 2017 SGR 1040) and URV projects (2018PFR-URV-B2-91). The Institut Català de Paleoecologia Humana i Evolució Social (IPHES-CERCA) has received financial support from the Spanish Ministry of Science and Innovation through the María de Maeztu program for Units of Excellence (CEX2019-000945-M).

**References**

Acovitsioti-hameau, A., Brochier, J.E., Hameau, P. (1999). Témoignages et marqueurs du pastoralisme actuel en grece: une ethnographie des gestes et des restes et les applications archaeologiques correlees. *Ethnologhia* 6–7, 93–135.

Albert, R.M., Shahack-Gross, R., Cabanes, D., Gilboa, A., Lev-Yadun, S., Portillo, M., Sharon, I., Boaretto, E., Weiner, S. (2008). Phytolith-rich layers from the Late Bronze and Iron Ages at Tel Dor (Israel): mode of formation and archaeological significance. *Journal of Archaeological Science* 35, 57–75. https://doi.org/10.1016/j.jas.2007.02.015

Angelucci, D.E., Boschian, G., Fontanals, M., Pedrotti, A., Vergès, J.-M. (2009). Shepherds and karst: the use of caves and rock-shelters in the Mediterranean region during the Neolithic. *Word Archaeology* 41, 191–214.

Bayarı, S.H., Özdemir, K., Sen, E.H., Araujo-606 Andrade, C., Erdal, Y.S., (2020). Application of ATR-FTIR spectroscopy and chemometrics for the discrimination of human bone remains from different archaeological sites in Turkey. Spectrochim. Acta - Part A Mol. *Biomol. Spectrosc*. 237. https://doi.org/10.1016/j.saa.2020.118311

Berzina-Cimdina, L., Borodajenko, N. (2012). Research of calcium phosphates using FTIR spectroscopy. Infrared Spectrosc. - *Mater. Sci. Eng. Technol*. 12, 251–263.

Bobroff, V., Chen, H.H., Javerzat, S., Petibois, C. (2016). What can infrared spectroscopy do for characterizing organic remnant in fossils? *TrAC - Trends Anal. Chem*. 82, 443–456. https://doi.org/10.1016/j.trac.2016.07.005

Botella López, M.C., Alemán Aguilera, I., Jiménez Brobeil, S.A. (2000). *Los Huesos Humanos: Manipulación y Alteraciones*. Barcelona, Ediciones Bellaterra.

Bradák, B., Carrancho, Á., Herrejón Lagunilla, Á., Villalaín, J. J., Monnier, G. F., Tostevin, G., et al. (2020). Magnetic fabric and archaeomagnetic analyses of anthropogenic ash horizons in a cave sediment succession (Crvena Stijena site, Montenegro). *Geophysical Journal International*, 224(2), 795–812. https://doi.org/10.1093/gji/ggaa461

Brochier, J.E. (1983). Combustion et parcage des herbivores domestiques. Le point de vue du sedimentologue. *Bulletin de la Société préhistorique français* 80, :143-145.

Brochier, J.E. (1991). Géoarchéologie du monde agropastoral, in: *Pour Une Archéologie Agraire*. À La Croisée Des Sciences de l'homme et de La Nature. Armand Colin Éditeur, Paris, pp. 303–322.

Brochier, J.É. (2005). Des hommes et des bêtes : une approche naturaliste de l'histoire et des pratiques de l'élevage, in: Guilaine, J. (Ed.), *Populations Néolithiques et Environnements*. Errance, pp. 137–152.

Brochier, J.E., Villa, P., Giacomarra, M., Tagliacozzo, A. (1992). Shepherds and sediments: Geo-ethnoarchaeology of pastoral sites. *Journal of Anthropological Archaeology* 11, 47–102. https://doi.org/10.1016/0278-4165(92)90010-9

Brönnimann, D., Ismail-Meyer, K., Rentzel, P., Pümpin, C., Lisá, L. (2017). Excrements of Herbivores, in: Nicosia, C., Stoops, G. (Eds.), *Archaeological Soil and Sediment Micromorphology*. John Wiley & Sons, Ltd, Chichester, UK, pp. 55–65. https://doi.org/10.1002/9781118941065.ch6

Bryant, V. M., Holloway, R. G. (1983). The role of palynology in archaeology. *Advances in Archaeological Method and Theory* 6: 191–224.

Bryant, V. M., Holloway, R. G. (1996). Chapter 23A. New frontiers in Palynology. In: Jansonius, J. y McGregror, D. C. (Eds). *Archaeological Palynology. Palynology: principles and applications*. American Association of Stratigraphic Palynologists Foundation. 3: 913- 917. Salt Lake City, Utah.

Bryant, V. M., Holloway, R. G., Jones, J. G., Carlson, D. L. (1994). Pollen preservation in alkaline soils of the American Southwest. In: Traverse, A. (Ed). *Sedimentation of organic particles*. Cambridge: Cambridge University Press, pp. 47–58.

Burguet-Coca, A. (2020). El fuego en la Prehistoria. *Una aproximación arqueo-experimental al registro piroarqueológico a través de la microarqueología.* Universitat Rovira i Virgili, Tarragona.

Burguet-Coca, A., Expósito, I. (2018). Construyendo un redil; tras el rastro de los microrrestos vegetales de un" *fumier*" experimental. *Butlleti Arqueològic* (Experiemental archaeology: from research to society: Proceedings of the Vth International Congress of Experimental Archaeology) 187–194.

Burguet-Coca, A., Polo-Díaz, A., Martínez-Moreno, J., Benito-Calvo, A., Allué, E., Mora, R., Cabanes, D. (2020). Pen management and livestock activities

based on phytoliths, dung spherulites, and minerals from Cova Gran de Santa Linya (Southeastern pre-Pyrenees). *Archaeological and Anthropological Sciences* 12. https://doi.org/10.1007/s12520-020-01101-6

Cabanes, D., Allué, E., Vallverdú, J., Cáceres, I., Vaquero, M., Pastó, I. (2007). Hearth structure and function at level J (50 kyr, BP) from Abric Romani (Capellades, Spain): phytolith, charcoal, bones and stone-tools (Part 3: Applications in Archaeology). In: Madella, M., Zurro, D. (Eds.). *Plants, People and Places: Recent studies in Phytolithic analysis*. Oxbow Books, Oxford, pp. 98–106.

Cáceres, I., (2002). *Tafonomía de yacimientos antrópicos en karst. Complejo Galería (Sierra de Atapuerca, burgos), Vanguard cave (Gibraltar) y Abric Romaní (Capellades, Barcelona).* Universitat Rovira i Virgili.

Cáceres, I., Lozano, M. and Saladié, P., (2007). Evidence for Bronze Age Cannibalism in El Mirador Cave (Sierra de Atapuerca, Burgos, Spain). *Am. J. Phys. Anthropol.* 133, 899–917. https://doi.org/10.1002/ajpa

Campbell, I. D. (1991). Experimental mechanical destruction of pollen grains. *Palynology* 15: 29–33.

Campbell, I. D. (1999). Quaternary pollen taphonomy: examples of differential redeposition and differential preservation. *Palaeogeography, Palaeoclimatology, Palaeoecology* 149: 245–256.

Campbell, I. D., Campbell, S. (1994). Pollen preservation: experimental wet–dry cycles in saline and desalinated sediments. Palynology 18: 5–10.

Canti, M.G., (1999). The Production and Preservation of Fecal Spherulites: Animals, Environment and Taphonomy. *Journal of Archaeological Science* 26, 251–258. http://dx.doi.org/10.1006/jasc.1998.0322

Canti, M.G., Brochier, J.É. (2017). Plant Ash, in: Nicosia, C., Stoops, G. (Eds.), *Archaeological Soil and Sediment Micromorphology*. John Wiley & Sons, Ltd, Chichester, UK, pp. 147–154. https://doi.org/10.1002/9781118941065.ch17

Carrancho, Á., Villalaín, J. J., Angelucci, D. E., Dekkers, M. J., Vallverdú, J., & Vergés, J. M. (2009). Rock-magnetic analyses as a tool to investigate archaeological fired sediments: A case study of Mirador cave (Sierra de Atapuerca, Spain). *Geophysical Journal International*, 179(1), 79–96. https://doi.org/10.1111/j.1365-246X.2009.04276.x

Carrancho, Á., Villalaín, J. J., Pavón-Carrasco, F. J., Osete, M. L., Straus, L. G., Vergès, J. M., Carretero, J. M., Angelucci, D.E., González Morales, M. R., Arsuaga, J. L., Bermúdez de Castro, J. M., and Carbonell, E. (2013). First directional European palaeosecular variation curve for the Neolithic based on archaeomagnetic data. Earth and Planetary Science Letters, 380, 124–37.

Chadefaux, C., Hô, A. Le, Bellot-gurlet, L., Ina, R. (2009). Curve-Fitting Micro-Atr-Ftir Studies of the Amide I and Ii Bands of Type I Collagen in. e-PRESERVATIONScience 129–137.

Coles, G. M., Gilbertson, D. D., Hunt, C. O., Jenkinson, R. D. S. (1989). Taphonomy and the palynology of cave deposits. *Cave Science* 16: 83-89.

Cushing, E. J. (1967). Evidence for differential pollen preservation in Late Quaternary sediments in Minnesota. *Review of Palaeobotany and Palynology* 4: 87–101.

Dal Sasso, G., Lebon, M., Angelini, I., Maritan, L., Usai, D., Artioli, G. (2016). Bone diagenesis variability among multiple burial phases at Al Khiday (Sudan) investigated by ATR-FTIR spectroscopy. *Palaeogeogr. Palaeoclimatol. Palaeoecol.* 463, 168–179. https://doi.org/10.1016/j.palaeo.2016.10.005

del Valle, H. (2018). *Aproximación a la Diagénesis del hueso en contextos de fumier: La Cueva de El Mirador (Sierra de Atapuerca, Burgos)* (Tesis de Máster). Universitat Rovira i Virgila, Tarragona.

Del Valle, H., Cáceres, I., Tornero, C., Burguet-Coca, A., Moclán, A., Vergès, J.M. (under review) ATR-FTIR to distinguish Holocene *fumier* facies. A perspective from bone diagenesis at El Mirador cave (Sierra de Atapuerca, Spain). *Journal of Archaeological Science, 141, 105582. https://doi.org/10.1016/j.jas.2022.105582*

Delhon, C., Martin, L., Argant, J., Thiébault, S. (2008). Shepherds and plants in the Alps: multi-proxy archaeobotanical analysis of neolithic dung from “La Grande Rivoire” (Isère, France). *Journal of Archaeological Science* 35, 2937–2952. https://doi.org/10.1016/j.jas.2008.06.007

Dimbleby, G. W. (1957). Pollen analysis of terrestrial soils. *New Phytologist* 56: 12–28.

Diot, M.-F. (1991). Apport et conservation sporo-pollinique dans les grottes: relationavec la frequentation humaine et animale. In: *Archaeologie Experimentale. Tome 2 e La Terre*. Editions Errance, Paris, pp. 236–245.

Égüez, N., Mallol, C., Martín-Socas, D., Camalich, M.D. (2016). Radiometric dates and micromorphological evidence for synchronous domestic activity and sheep penning in a Neolithic cave: Cueva de El Toro (Málaga, Antequera, Spain). *Archaeological and Anthropological Sciences* 8, 107–123. https://doi.org/10.1007/s12520-014-0217-0

Ellingham, S.T.D., Thompson, T.J.U., Islam, M. (2016). The Effect of Soft Tissue on Temperature Estimation from Burnt Bone Using Fourier Transform Infrared Spectroscopy. *J. Forensic Sci*. 61, 153–159. https://doi.org/10.1111/1556-4029.12855

Expósito, I., Burjachs, F. (2016). Taphonomic approach to the palynological record of burnt and unburnt samples from El Mirador Cave (Sierra de Atapuerca, Burgos, Spain). *Quaternary International* 414, 258–271. https://doi.org/10.1016/j.quaint.2016.01.051

Fernández-López, S. R. (1995). Taphonomie et interprétation des paléoenvironnements. *Geobios, mémoire spécial* 18: 137–154.

Friesem, D.E. (2016). Geo-ethnoarchaeology in action. *Journal of Archaeological Science* 70, 145–157. https://doi.org/10.1016/j.jas.2016.05.004

Ghosh, R., D’Rozario, A., Bera, S. (2006). Can palynomorphs occur in burnt ancient potsherds? An experimental proof. *Journal of Archaeological Science* 33: 1445–1451.

Goldberg, P., Macphail, R.I. (2006). *Practical and Theoretical Geoarchaeology*. Blackwell publishing, Victoria.

Gur-Arieh S, Shahack-Gross R, Maeir AM, et al (2014) The taphonomy and preservation of wood and dung ashes found in archaeological cooking installations: case studies from Iron Age Israel. *Journal of Archaeological Science* 46:50–67. https://doi.org/10.1016/j.jas.2014.03.011

Havinga, A. (1967). Palynology and pollen preservation. *Review of Palaeobotany and Palynology* 2: 81–98.

Havinga, A. (1971). An experimental investigation into the decay of pollen and spores in various soil types. In: Brooks, L. (Ed*). Sporopollenin*. Academic Press. New York: 446–479.

Hedges, R.E.M. (2002). Bone Diagenesis: an Overview of Processes. Archaeometry 44, 319–328.

Herrejón-Lagunilla, Á., Carrancho, Á., Villalaín, J. (this book). On the suitability of prehistoric anthropogenic burnt sediments (*fumiers*) for archaeomagnetic studies at El Mirador cave (Burgos, Spain). In P. Martín, J.M. Vergès, E. Allué (Eds.) Prehistoric Herders and Farmers - A Transdisciplinary Overview of the Archaeological Record from El Mirador Cave. Interdisciplinary Contributions to Archaeology, Springer.

Holloway, R. G. (1989). Experimental mechanical pollen degradation and its application to Quaternary age deposits. *Tex. J. Sci.* 41: 131–145.

Horowitz, A. (1992). *Palynology of Arid Lands*. Elsevier. Amsterdam.

Jelinek, V. (1981). *Characterization of the magnetic fabric of rocks. Tectonophysics*, 79(3–4), 63–67. https://doi.org/10.1016/0040-1951(81)90110-4

Karkanas, P., Bar-Yosef, O., Goldberg, P., Weiner, S. (2000). Diagenesis in Prehistoric Caves: The Use of Minerals that Form In Situ to Assess the Completeness of the Archaeological Record. *Journal of Archaeological Science* 27, 915–929. https://doi.org/10.1006/jasc.1999.0506

Koon, H.E.C., Nicholson, R.A., Collins, M.J. (2003). A practical approach to the identification of low temperature heated bone using TEM. *J. Archaeol. Sci*. 30, 1393–1399. https://doi.org/10.1016/S0305-4403(03)00034-7

Koon, H.E.C., O'Connor, T.P., Collins, M.J. (2010). Sorting the butchered from the boiled. *J. Archaeol. Sci.* 37, 62–69. https://doi.org/10.1016/j.jas.2009.08.015

Lebon, M., Reiche, I., Bahain, J.J., Chadefaux, C., Moigne, A.M., Fröhlich, F., Sémah, F., Schwarcz, H.P., Falguères, C. (2010). New parameters for the characterization of diagenetic alterations and heat-induced changes of fossil bone mineral using Fourier transform infrared spectrometry. *J. Archaeol. Sci.* 37, 2265–2276. https://doi.org/10.1016/j.jas.2010.03.024

Lebreton, V., Messager, E., Marquer, L., Renault-Miskovsky, J. (2010). A neotaphonomic experiment in pollen oxidation and its implications for archaeopalynology. *Review of Palaeobotany and Palynology* 162: 29–38.

Leskovar, T., Zupanič Pajnič, I., Geršak, Ž.M., Jerman, I., Črešnar, M. (2020). ATR-FTIR spectroscopy combined with data manipulation as a pre-screening method to assess DNA preservation in skeletal remains. *Forensic Sci. Int. Genet*. 44, 102196. https://doi.org/10.1016/j.fsigen.2019.102196

Macphail, R.I., Courty, M.-A., Hather, J., Wattez, J., Ryder, M., Cameron, N., Branch, N.P. (1997). The soil micromorphological evidence of domestic occupation and stabling activities, in: Maggi, R. (Ed.), *Arene Candide: A Functional and Environmental Assessment of the Holocene Sequence (Excavations Bernarbo' Brea-Cardini 1940–50).* Il Calamo, Roma, pp. 53–88.

Mallol, C., Mentzer, S. M., & Miller, C. E. (2017). Combustion Features. In *Archaeological Soil and Sediment Micromorphology* (pp. 299–330). Wiley Online Library.

Marques, M.P.M., Mamede, A.P., Vassalo, A.R., Makhoul, C., Cunha, E., Gonçalves, D., Parker, S.F., Batista de Carvalho, L.A.E. (2018). Heat-induced Bone Diagenesis Probed by Vibrational Spectroscopy. *Sci. Rep.* 8, 1–13. https://doi.org/10.1038/s41598-018-34376-w

Martín-Rodríguez, P., Vergès, J.M. (2016). Bone alterations in *fumier*s: Experimental approach. *Quaternary International* 414, 294–303. https://doi.org/10.1016/j.quaint.2015.12.056

Matthews, W. (2010). Geoarchaeology and taphonomy of plant remains and microarchaeological residues in early urban environments in the Ancient Near East. *Quaternary International* 214, 98–113. http://dx.doi.org/10.1016/j.quaint.2009.10.019

McClean, R. G., & Kean, W. F. (1993). Contributions of wood ash magnetism to archaeomagnetic properties of fire pits and hearths. *Earth and Planetary Science Letters,* 119(3), 387–394.

Munro, L.E., Longstaffe, F.J., White, C.D. (2007). Burning and boiling of modern deer bone: Effects on crystallinity and oxygen isotope composition of bioapatite phosphate. *Paleogeography, Paleoclimatology, Paleoecol*. 249, 90–102. https://doi.org/10.1016/j.palaeo.2007.01.011

Nicholson, R.A. (1996). Bone degradation, burial medium and species representation: Debunking the myths, an experiment-based approach. *J. Archaeol. Sci.* 23, 513–533. https://doi.org/10.1006/jasc.1996.0049

Nicholson, R.A. (1998). Bone degradation in a compost heap. *J. Archaeol. Sci.* 25, 393–403. https://doi.org/10.1006/jasc.1997.0208

Panadès, X., Bartolomé, J., Strömberg, C., Soriano, I., Buckland, P., Serieyssol, K.K., Bach, J., Arillo, A., Lozar, F., Stevenson, T., Chamorro, L., Ditchfiels, P. (2016). The utility of livestock dung for reconstructing recent ethnological and environmental histories. *Environmental Archaeology.* https://doi.org/10.1080/14614103.2016.1142630

Peters, C., Church, M. J., & Mitchell, C. (2001). Investigation of fire ash residues using mineral magnetism. *Archaeological Prospection*, 8(4), 227–237. https://doi.org/10.1002/arp.171

Pijoan, C.M., Mansilla, J., Leboreiro, I., Lara, V.H., Bosch, P. (2007). Thermal alterations in archaeological bones. *Archaeometry* 49, 713–727. https://doi.org/10.1111/j.1475-4754.2007.00331.x

Piperno, D.R. (2006). *Phytoliths: A comprehensive guide for archaeologists and paleoecologists.* AltaMira Press, Lanham.

Polo-Díaz, A., Alonso Eguíluz, M., Ruiz, M., Pérez, S., Mújika, J., Albert, R.M., Fernández Eraso, J. (2016). Management of residues and natural resources at San Cristóbal rock-shelter: Contribution to the characterisation of chalcolithic agropastoral groups in the Iberian Peninsula. *Quaternary International* 414, 202–225. https://doi.org/10.1016/j.quaint.2016.02.013

Polo-Díaz, A., Martínez-Moreno, J., Benito-Calvo, A., Mora, R. (2014). Prehistoric herding facilities: site formation processes and archaeological dynamics in Cova Gran de Santa Linya (Southeastern Prepyrenees, Iberia). *Journal of Archaeological Science* 41, 784–800. https://doi.org/10.1016/j.jas.2013.09.013

Portillo, M., Albert, R.M. (2011). Husbandry practices and livestock dung at the Numidian site of Althiburos (el Médéina, Kef Governorate, northern Tunisia): the phytolith and spherulite evidence. *Journal of Archaeological Science* 38, 3224–3233. https://doi.org/10.1016/j.jas.2011.06.027

Roberts, S.J., Smith, C.I., Millard, A., Collins, M.J. (2002). The Taphonomy of cooked bone: Characterizing boiling and its physuco-chemical effects. *Archaeometry* 44, 485–494.

Sangster, A. G., Dale, H. M. (1961). A preliminary study of differential pollen grain preservation. *Canadian Journal of Botany* 39: 35–43.

Shahack-Gross R (2011) Herbivorous livestock dung: formation, taphonomy, methods for identification, and archaeological significance. *Journal of Archaeological Science* 38:205–218. https://doi.org/10.1016/j.jas.2010.09.019

Shahack-Gross, R., Albert, R.M., Gilboa, A., Nagar-Hilman, O., Sharon, I., Weiner, L. (2005). Geoarchaeology in an urban context: The uses of space in a

Phoenician monumental building at Tel Dor (Israel). *Journal of Archaeological Science* 32, 1417–1431.

Shahack-Gross, R., Marshall, F., Weiner, S. (2003). Geo-Ethnoarchaeology of Pastoral Sites: The Identification of Livestock Enclosures in Abandoned Maasai Settlements. *Journal of Archaeological Science* 30, 439–459. https://doi.org/10.1006/jasc.2002.0853

Simpson, D. J., Hunt, C. O. (2009). Scoping the past human environment: a case study of pollen taphonomy at the Haua Fteah, Cyrenaica, Lybia. *Arch. Rev. Camb*. 24: 27–46.

Tarling, D. H., & Hrouda, F. (1993). *The magnetic anisotropy of rocks*. London: Chapman & Hall.

Tian, F., Cao, X., Xu, Q., Li, Y. (2009). A laboratorial study on influence of alkaline and oxidative environment on preservation of Pinus tabulaeformis pollen. *Front. Earth Sci.* China 3 (2): 226–230.

Twiddle, C. L., Bunting, M. J. (2010). Experimental investigations into the preservation of pollen grains: A pilot study of four pollen types. *Review of Palaeobotany and Palynology* 162: 621–630.

Vergès, J.-M. (2011). La combustión del estiércol: aproximación experimetal a la quema en montón de los residuos de redil, in: Morgado, A., Baena, J., García-González, D. (Eds.), *La Investigación Experimental Aplicada a La Arqueología*. Editorial Universidad de Granada, Granada, pp. 325–330.

Vergès, J.M., Allué, E., Fontanals, M., Morales, J.I., Martín, P., Carrancho, Á., Expósito, I., Guardiola, M., Lozano, M., Marsal, R., Oms, X., Euba, I., Rodríguez, A. (2016a). El Mirador cave (Sierra de Atapuerca, Burgos, Spain): A whole perspective. *Quaternary International* 414, 236–243. https://doi.org/10.1016/j.quaint.2016.01.044

Vergès, J.M., Burguet-Coca, A., Allué, E., Expósito, I., Guardiola, M., Martín, P., Morales, J.I., Burjachs, F., Cabanes, D., Carrancho, Á., Vallverdú, J. (2016b). The Mas del Pepet experimental programme for the study of prehistoric

livestock practices: Preliminary data from dung burning. *Quaternary International* 414, 304–315. https://doi.org/10.1016/j.quaint.2016.01.032

Weiner, S. (2010). *Microarchaeology. Beyond the Visible Archaeological Record*. Cambridge University Press, New York.

Weinstein-Evron, M. (1981). The influence of slope direction on the pollen spectra. *Pollen et Spores* 23 (3): 381–387.

Weinstein-Evron, M. (1994). Biases in archaeological pollen assemblages. Aspects of Archaeological Palynology: Methodology and Applications. O. K. Davis. *American Association of Stratigraphic Palynologists Contributions Series*. 29: 193–205.

White, T.D. (1992). *Prehistoric Cannibalism at Mancos* 5MTUMR-2346 Princeton: Univ. Press, Princeton, NJ.

**Figures and table captions**

**Fig. 1 a.** Example of ATR-FTIR spectra of bone samples from facies and assignments of the main bands. **b.** Sediment spectra of some of the studied samples. MIR104-187 facies *b*; MIR104-103 facies *c*; MIR105-106 facies *a*; MIR105-101 facies *a*

**Fig. 2** Results of anisotropy of magnetic susceptibility (AMS) for the burning events Ci2 and Ci3 (level MIR 104), Ci5, Ci6 and Ci7 (level MIR107), ordered according to their relative stratigraphic position (Ci2 is the shallowest, and Ci7 the deepest). All of them were located in Sector 100. The graphics correspond to Equal area projection of the magnetic ellipsoid axes (left), corrected anisotropy degree [PJ] vs. magnetic susceptibility [Km] plot (center) and shape parameter [T] vs. PJ plot (right). In the equal area projection plot, K1 = blue squares, K2 = green triangles and K3 = pink circles (small symbols show the results for each specimen, and large symbols represent the mean direction). Confidence ellipses (95%) are also shown. **Fig. 3 a-b**. Hysteresis loops and **c-d**. thermomagnetic curves (temperature vs. magnetization) of white facies from Ci2 event (level MIR104). Pannel **e**. shows the white patch inside Ci2.**Table 1** Statistical parameters of the anisotropy of magnetic susceptibility (AMS) (N=

number of samples considered for the calculations / N'= total number of measured samples/ St. D = Standard deviation / $K_m$= susceptibility value / L= magnetic lineation / F= magnetic foliation / $P_J$= corrected anisotropy degree / T= shape parameter)

**Supplementary information 1** Materials

**Supplementary information 2** Methods

**Supplementary information 3** Main diagenetic parameters through ATR-FTIR and thermal alterations

**Supplementary information 4** FTIR results from bulk samples

**Supplementary information 5** Phytoliths and dung spherulites results

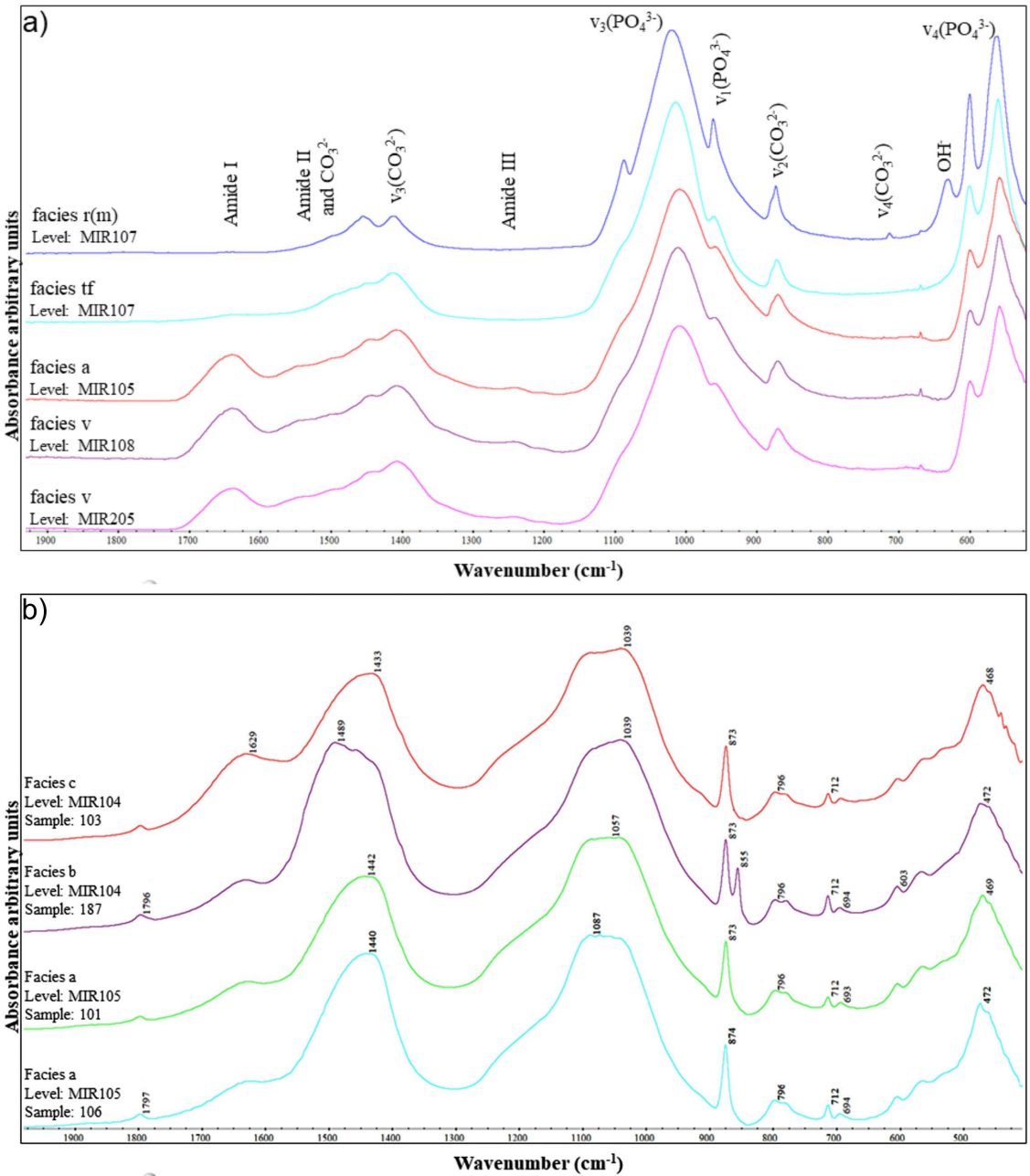
a)
Amide I
Amide II and $CO_3^{2-}$
$v_3(CO_3^{2-})$
Amide III
$v_3(PO_4^{3-})$
$v_1(PO_4^{3-})$
$v_2(CO_3^{2-})$
$v_4(CO_3^{2-})$
OH
$v_4(PO_4^{3-})$
facies r(m)
Level: MIR107
facies tf
Level: MIR107
facies a
Level: MIR105
facies v
Level: MIR108
facies v
Level: MIR205
Absorbance arbitrary units
Wavenumber ($cm^{-1}$)
b)
Facies c
Level: MIR104
Sample: 103
Facies b
Level: MIR104
Sample: 187
Facies a
Level: MIR105
Sample: 101
Facies a
Level: MIR105
Sample: 106
Absorbance arbitrary units
Wavenumber ($cm^{-1}$)

## a) Ci2

N/N'=7/8

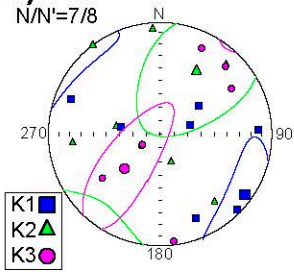


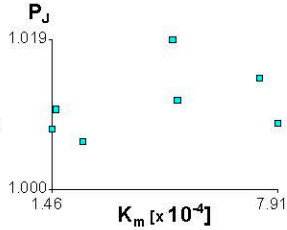


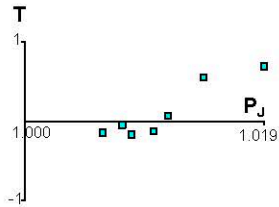


## b) Ci3

N/N'=12/13

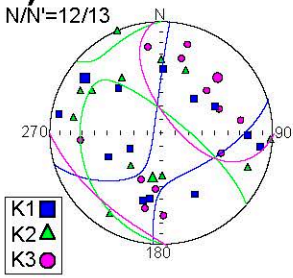


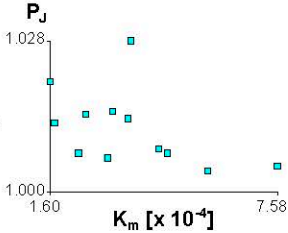


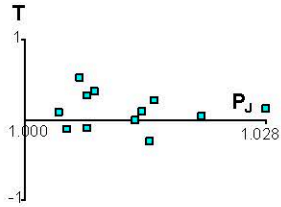


## c) Ci5

N/N'=13/13

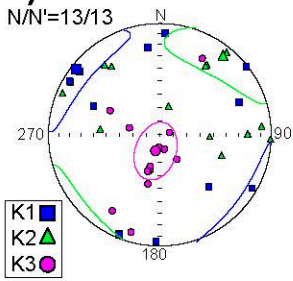


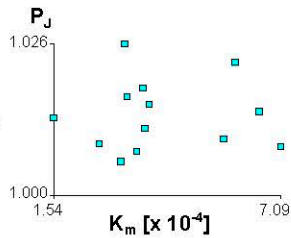


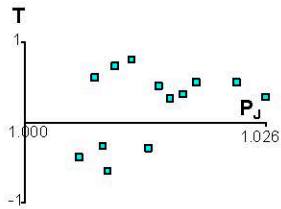


## d) Ci6

N/N'=11/12

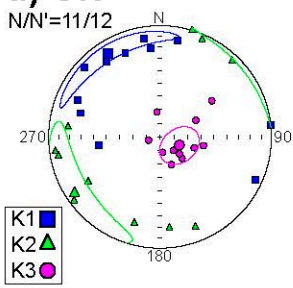


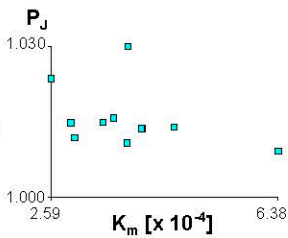


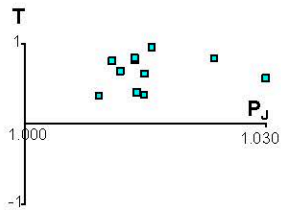


## e) Ci7

N/N'=10/10

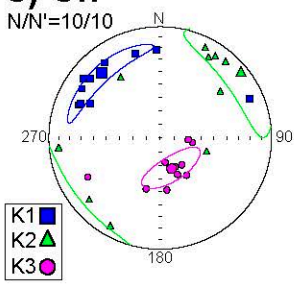


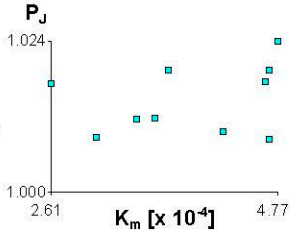


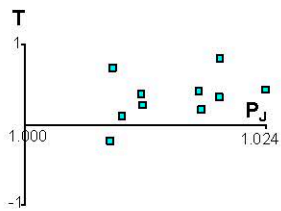

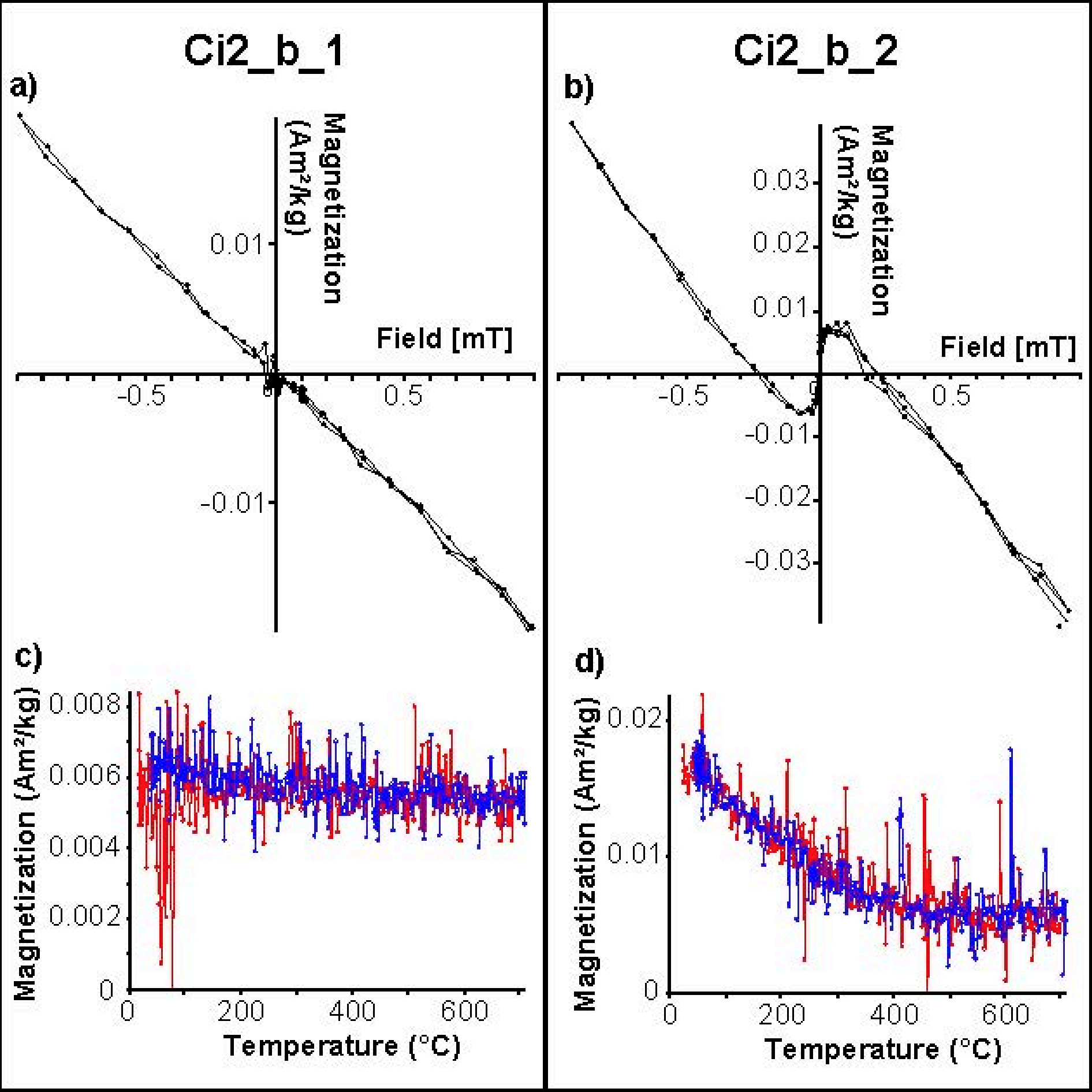
Ci2_b_1
a)
Magnetization (Am²/kg)
0.01
-0.01
Field [mT]
-0.5
0
0.5
Ci2_b_2
b)
Magnetization (Am²/kg)
0.03
0.02
0.01
-0.01
-0.02
-0.03
Field [mT]
-0.5
0
0.5
c)
Magnetization (Am²/kg)
0.008
0.006
0.004
0.002
0
0
200
400
600
Temperature (°C)
d)
Magnetization (Am²/kg)
0.02
0.01
0
0
200
400
600
Temperature (°C)

| Combustion episodes | N | N' | $K_m$ | | L | | | F | | | $P_J$ | | | T | | |
|---|---|---|---|---|---|---|---|---|---|---|---|---|---|---|---|---|
| | | | Average | Standard deviation | Mean | Average | Standard deviation | Mean | Average | Standard deviation | Mean | Average | St.D | Mean | Average | Standard deviation |
| Ci2 | 7 | 8 | 4.37E-04 | 2.67E-04 | 1,003 | 1,004 | 0.001 | 1,002 | 1,007 | 0.005 | 1,005 | 1,011 | 0 | -0.088 | 0.117 | 0.353 |
| Ci3 | 12 | 13 | 3.69E-04 | 1.73E-04 | 1,001 | 1,005 | 0.003 | 1,002 | 1,006 | 0.004 | 1,003 | 1,012 | 0.01 | 0.446 | 0.114 | 0.223 |
| Ci5 | 13 | 13 | 4.17E-04 | 1.64E-04 | 1,002 | 1,005 | 0.002 | 1,007 | 1,009 | 0.005 | 1,009 | 1,014 | 0.01 | 0.534 | 0.220 | 0.464 |
| Ci6 | 11 | 12 | 3.86E-04 | 1.03E-04 | 1,001 | 1,003 | 0.002 | 1,010 | 1,012 | 0.005 | 1,013 | 1,016 | 0.01 | 0.764 | 0.648 | 0.209 |
| Ci7 | 10 | 10 | 3.94E-04 | 7.76E-05 | 1,004 | 1,004 | 0.002 | 1,007 | 1,010 | 0.004 | 1,011 | 1,015 | 0.01 | 0.306 | 0.351 | 0.292 |

**CHAPTER 6: SUPPLEMENTARY MATERIAL**

**The fumier sequences of El Mirador: an approach to fire as a sociocultural practice and taphonomic agent.**

Burguet-Coca, A., del Valle, H., Expósito, I., Herrejón Lagunilla, A., Buitkute, E. Cabanes, D., Cáceres, I., Carrancho, A., Villalaín, J.J.

**Supplementary material 1 (SM 1): Materials**

| Type analysis | Level | Square | Num. | facies | Type sample | X | Y | ZINF |
|---|---|---|---|---|---|---|---|---|
| Phyt., Sph. | MIR104 | T15 | 188 | b | bulk sample | 95 | 32 | 1267 |
| Phyt., Sph. | MIR104 | T15 | 187 | b | bulk sample | 92 | 31 | 1274 |
| Phyt., Sph. | MIR104 | T15 | 185 | b | bulk sample | 89 | 57 | 1283 |
| Phyt., Sph. | MIR104 | T15 | 186 | c | bulk sample | 89 | 28 | 1287 |
| Phyt., Sph. | MIR104 | S15 | 104 | b | bulk sample | 92 | 57 | 1295 |
| Phyt., Sph. | MIR104 | S15 | 103 | c | bulk sample | 88 | 81 | 1305 |
| Phyt., Sph. | MIR105 | S15 | 108 | a | bulk sample | 83 | 82 | 1313 |
| Phyt., Sph. | MIR105 | S15 | 107 | a | bulk sample | 82 | 82 | 1322 |
| Phyt., Sph. | MIR105 | S15 | 106 | a | bulk sample | 83 | 85 | 1332 |
| Phyt., Sph. | MIR105 | S15 | 105 | a | bulk sample | 82 | 8 | 1342 |
| Phyt., Sph. | MIR105 | S15 | 104 | a | bulk sample | 81 | 82 | 1362 |
| Phyt., Sph. | MIR105 | S15 | 103 | a | bulk sample | 81 | 82 | 1374 |
| Phyt., Sph. | MIR105 | S15 | 102 | a | bulk sample | 82 | 84 | 1394 |
| Phyt., Sph. | MIR105 | S15 | 101 | a | bulk sample | 83 | 87 | 1404 |
| Phyt., Sph. | MIR105 | S15 | 100 | a | bulk sample | 85 | 86 | 1420 |
| FTIR | MIR 105 | T12 | 79 | a | bulk sample | 77 | 20 | 1536 |
| FTIR | MIR 105 | T12 | 130 | a | bulk sample | 16 | 35 | 1544 |
| FTIR | MIR 105 | T12 | 148 | a | bulk sample | 10 | 40 | 1544 |
| FTIR | MIR 105 | T12 | 154 | a | bulk sample | 51 | 48 | 1547 |
| FTIR | MIR 105 | T12 | 172 | a | bulk sample | 42 | 53 | 1555 |
| FTIR | MIR 105 | T12 | 177 | a | bulk sample | 68 | 25 | 1550 |
| FTIR | MIR 105 | T13 | 104 | a | bulk sample | 20 | 69 | 1530 |
| FTIR | MIR 105 | T13 | 121 | a | bulk sample | 25 | 47 | 1544 |
| FTIR | MIR 105 | T12 | 77 | a | bulk sample | 82 | 10 | 1536 |
| FTIR | MIR 105 | T12 | 175 | a | bulk sample | 28 | 83 | 1553 |
| FTIR | MIR 105 | V12 | 5 | a | bulk sample | 35 | 7 | 1520 |
| FTIR | MIR 108 | V12 | 18 | v | bulk sample | 94 | 76 | 1563 |
| FTIR | MIR 108 | V12 | 20 | v | bulk sample | 79 | 71 | 1561 |
| FTIR | MIR 108 | V12 | 6 | v | bulk sample | 97 | 29 | 1557 |
| FTIR | MIR 108 | V12 | 13 | v | bulk sample | 69 | 74 | 1561 |
| FTIR | MIR 108 | V12 | 16 | v | bulk sample | 85 | 70 | 1561 |
| FTIR | MIR 108 | V12 | 22 | v | bulk sample | 91 | 67 | 1561 |
| FTIR | MIR 108 | V12 | 24 | v | bulk sample | 90 | 62 | 1560 |
| FTIR | MIR 108 | V12 | 61 | v | bulk sample | 90 | 65 | 1565 |
| FTIR | MIR 108 | V13 | 50 | v | bulk sample | 65 | 85 | 1558 |
| FTIR | MIR 108 | W13 | 94 | v | bulk sample | 2 | 78 | 1560 |
| FTIR | MIR 108 | V13 | 64 | v | bulk sample | 60 | 62 | 1559 |
| FTIR | MIR 205 | O37 | 7 | v | bulk sample | 37 | 88 | 1331 |
| FTIR | MIR 205 | O37 | 10 | v | bulk sample | 42 | 0 | 1331 |
| FTIR | MIR 205 | O38 | 37 | v | bulk sample | 57 | 40 | 1341 |
| FTIR | MIR 205 | P36 | 19 | v | bulk sample | 82 | 60 | 1344 |
| FTIR | MIR 205 | P36 | 21 | v | bulk sample | 44 | 85 | 1335 |
| FTIR | MIR 205 | P38 | 26 | v | bulk sample | 21 | 95 | 1331 |
| FTIR | MIR 205 | Q37 | 27 | v | bulk sample | 35 | 34 | 1343 |
| FTIR | MIR 205 | Q37 | 36 | v | bulk sample | 51 | 6 | 1351 |
| FTIR | MIR 205 | Q38 | 29 | v | bulk sample | 38 | 57 | 1337 |
| FTIR | MIR 205 | Q38 | 54 | v | bulk sample | 54 | 72 | 1343 |
| FTIR | MIR 205 | O37 | 14 | v | bulk sample | 32 | 97 | 1335 |
| FTIR | MIR 107 | V13 | 195 | tf | bulk sample | 79 | 10 | 1537 |
| FTIR | MIR 107 | V13 | 197 | tf | bulk sample | 70 | 74 | 1537 |
| FTIR | MIR 107 | V13 | 201 | tf | bulk sample | 6 | 48 | 1537 |
| FTIR | MIR 107 | V13 | 202 | tf | bulk sample | 68 | 77 | 1537 |
| FTIR | MIR 107 | V13 | 204 | tf | bulk sample | 4 | 47 | 1537 |
| FTIR | MIR 107 | V13 | 212 | tf | bulk sample | 5 | 63 | 1539 |
| FTIR | MIR 107 | V13 | 215 | tf | bulk sample | 10 | 55 | 1540 |
| FTIR | MIR 107 | V13 | 218 | tf | bulk sample | 12 | 55 | 1542 |
| FTIR | MIR 107 | V13 | 226 | tf | bulk sample | 51 | 56 | 1541 |
| FTIR | MIR 107 | V13 | 228 | tf | bulk sample | 40 | 64 | 1542 |
| FTIR | MIR 107 | V13 | 208 | tf | bulk sample | 50 | 50 | 1545 |
| FTIR | MIR 107 | V13 | 98 | r(m) | bulk sample | 81 | 9 | 1513 |
| FTIR | MIR 107 | V13 | 99 | r(m) | bulk sample | 74 | 13 | 1514 |
| FTIR | MIR 107 | V13 | 114 | r(m) | bulk sample | 43 | 23 | 1511 |
| FTIR | MIR 107 | V13 | 116 | r(m) | bulk sample | 42 | 27 | 1510 |
| FTIR | MIR 107 | V13 | 105 | r(m) | bulk sample | 56 | 8 | 1513 |
| FTIR | MIR 107 | V14 | 209 | r(m) | bulk sample | 50 | 50 | 1520 |
| FTIR | MIR 105 | T13 | 103 | a | bone | 30 | 53 | 1529 |
| FTIR | MIR 105 | T12 | 76 | a | bone | 82 | 10 | 1536 |
| FTIR | MIR 105 | T12 | 78 | a | bone | 77 | 20 | 1536 |
| FTIR | MIR 105 | T13 | 122 | a | bone | 60 | 30 | 1545 |
| FTIR | MIR 105 | T12 | 129 | a | bone | 16 | 35 | 1544 |
| FTIR | MIR 105 | T12 | 147 | a | bone | 10 | 40 | 1544 |
| FTIR | MIR 105 | T12 | 153 | a | bone | 51 | 48 | 1547 |

| | | | | | | | | |
|---|---|---|---|---|---|---|---|---|
| FTIR | MIR 105 | T12 | 171 | a | bone | 42 | 73 | 1554 |
| FTIR | MIR 105 | T12 | 174 | a | bone | 28 | 83 | 1552 |
| FTIR | MIR 105 | T12 | 176 | a | bone | 68 | 25 | 1549 |
| FTIR | MIR 108 | V12 | 17 | v | bone | 93 | 75 | 1562 |
| FTIR | MIR 108 | V12 | 21 | v | bone | 92 | 68 | 1560 |
| FTIR | MIR 108 | V12 | 15 | v | bone | 86 | 69 | 1560 |
| FTIR | MIR 108 | V12 | 60 | v | bone | 89 | 75 | 1564 |
| FTIR | MIR 108 | V13 | 93 | v | bone | 1 | 77 | 1559 |
| FTIR | MIR 108 | V12 | 19 | v | bone | 80 | 72 | 1561 |
| FTIR | MIR 108 | V12 | 5 | v | bone | 98 | 28 | 1556 |
| FTIR | MIR 108 | V12 | 23 | v | bone | 91 | 61 | 1559 |
| FTIR | MIR 108 | V13 | 49 | v | bone | 64 | 84 | 1557 |
| FTIR | MIR 108 | V12 | 12 | v | bone | 80 | 73 | 1560 |
| FTIR | MIR 205 | Q37 | 35 | v | bone | 50 | 6 | 1351 |
| FTIR | MIR 205 | O38 | 36 | v | bone | 58 | 42 | 1341 |
| FTIR | MIR 205 | Q38 | 53 | v | bone | 24 | 72 | 1343 |
| FTIR | MIR 205 | Q38 | 28 | v | bone | 48 | 57 | 1337 |
| FTIR | MIR 205 | 037 | 6 | v | bone | 37 | 88 | 1331 |
| FTIR | MIR 205 | P36 | 20 | v | bone | 44 | 85 | 1335 |
| FTIR | MIR 205 | P38 | 25 | v | bone | 22 | 95 | 1330 |
| FTIR | MIR 205 | O37 | 9 | v | bone | 42 | 0 | 1331 |
| FTIR | MIR 205 | P36 | 18 | v | bone | 82 | 60 | 1344 |
| FTIR | MIR 205 | Q37 | 26 | v | bone | 35 | 33 | 1342 |
| FTIR | MIR 107 | V13 | 54 | tf | bone | 71 | 73 | 1537 |
| FTIR | MIR 107 | V13 | 35 | tf | bone | 5 | 62 | 1505 |
| FTIR | MIR 107 | V13 | 66 | tf | bone | 4 | 48 | 1537 |
| FTIR | MIR 107 | V13 | 77 | tf | bone | 11 | 57 | 1540 |
| FTIR | MIR 107 | V13 | 59 | tf | bone | 5 | 51 | 1538 |
| FTIR | MIR 107 | V13 | 45 | tf | bone | 80 | 9 | 1536 |
| FTIR | MIR 107 | V13 | 19 | tf | bone | 52 | 57 | 1541 |
| FTIR | MIR 107 | V13 | 52 | tf | bone | 39 | 65 | 1542 |
| FTIR | MIR 107 | V13 | 43 | tf | bone | 23 | 35 | 1542 |
| FTIR | MIR 107 | V13 | 46 | tf | bone | 69 | 75 | 1536 |
| FTIR | MIR 107 | V13 | 113 | r(m) | bone | 43 | 23 | 1511 |
| FTIR | MIR 107 | V13 | 97 | r(m) | bone | 74 | 13 | 1514 |
| FTIR | MIR 107 | V13 | 104 | r(m) | bone | 56 | 8 | 1513 |
| FTIR | MIR 107 | V13 | 92 | r(m) | bone | 81 | 9 | 1513 |
| FTIR | MIR 107 | V13 | 115 | r(m) | bone | 42 | 27 | 1510 |
| Paleoparasitology | MIR208 | Q38 | 1 | v | bulk sample | 12 | 42 | 1377 |
| Paleoparasitology | MIR208 | O38 | 19 | v | bulk sample | 14 | 52 | 1388 |
| Paleoparasitology | MIR208 | Q37 | 16 | m | bulk sample | 69 | 16 | 1382 |
| Paleoparasitology | MIR208 | P37 | 41 | m | bulk sample | 66 | 36 | 1391 |
| Paleoparasitology | MIR208 | O39 | 23 | m | bulk sample | 9 | 87 | 1373 |
| Paleoparasitology | MIR107 | V14 | 43 | tf | bulk sample | 72 | 5 | 1485 |
| Paleoparasitology | MIR107 | V14 | 44 | c | bulk sample | 67 | 8 | 1492 |
| Paleoparasitology | MIR107 | V14 | 46 | m | bulk sample | 68 | 8 | 1494 |
| Paleoparasitology | MIR107 | V14 | 47 | bg | bulk sample | 73 | 32 | 1493 |
| Paleoparasitology | MIR107 | V14 | 48 | tf | bulk sample | 74 | 26 | 1499 |
| Paleoparasitology | MIR107 | V14 | 50 | c | bulk sample | 20 | 32 | 1513 |
| Paleoparasitology | MIR107 | V14 | 59 | m | bulk sample | 40 | 47 | 1517 |
| Paleoparasitology | MIR107 | V14 | 60 | tf | bulk sample | 32 | 35 | 1520 |
| Paleoparasitology | MIR108 | V14 | 74 | v | bulk sample | 67 | 10 | 1567 |
| Paleoparasitology | MIR107 | V14 | 90 | c | bulk sample | 9 | 54 | 1535 |
| Paleoparasitology | MIR107 | V14 | 119 | tf | bulk sample | 12 | 42 | 1550 |
| Paleoparasitology | MIR107 | V14 | 127 | m | bulk sample | 12 | 67 | 1548 |
| Paleoparasitology | MIR107 | V14 | 128 | a | bulk sample | 23 | 52 | 1551 |
| Paleoparasitology | MIR107 | V14 | 141 | f | bulk sample | 46 | 80 | 1562 |
| Paleoparasitology | MIR107 | V14 | 142 | c | bulk sample | 23 | 31 | 1555 |
| Archaeomagnetism | MIR103 | | Ci2 Grey ash facies 1 | Grey ash facies | bulk sample | - | - | - |
| Archaeomagnetism | MIR103 | | Ci2 Grey ash facies 2 | Grey ash facies | bulk sample | - | - | - |
| Archaeomagnetism | MIR103 | | Ci2 White facies | White facies | bulk sample | - | - | - |
| Archaeomagnetism | MIR103 | | Ci2 Carbonaceous facies | Carbonaceous facies | bulk sample | - | - | - |
| Archaeomagnetism | MIR103 | | Ci2-59 | Carbonaceous facies | bulk sample | - | - | - |
| Archaeomagnetism | MIR103 | | Ci2-60 | Carbonaceous facies | bulk sample | - | - | - |
| Archaeomagnetism | MIR103 | | Ci3 Ash facies | Ash facies | bulk sample | - | - | - |
| Archaeomagnetism | MIR103 | | Ci3 Grey ash facies | Grey ash facies | bulk sample | - | - | - |
| Archaeomagnetism | MIR103 | | Ci3 Carbonaceous facies | Carbonaceous facies | bulk sample | - | - | - |
| Archaeomagnetism | MIR107 | | Ci6-1 | Ash facies | bulk sample | - | - | - |
| Archaeomagnetism | MIR107 | | Ci6-3 | Ash facies | bulk sample | - | - | - |
| Archaeomagnetism | MIR107 | | Ci6-4 | Ash facies | bulk sample | - | - | - |
| Archaeomagnetism | MIR107 | | Ci6-7 | Ash facies | bulk sample | - | - | - |
| Archaeomagnetism | MIR107 | | Ci6-8 | Ash facies | bulk sample | - | - | - |
| Archaeomagnetism | MIR107 | | Ci6-9 | Ash facies | bulk sample | - | - | - |
| Archaeomagnetism | MIR107 | | Ci6-12 | Ash facies | bulk sample | - | - | - |
| Archaeomagnetism | MIR107 | | Ci5-1 | Ash facies | bulk sample | - | - | - |

| | | | | | | | | |
|---|---|---|---|---|---|---|---|---|
| Archaeomagnetism | MIR107 | | Ci5-2 | Ash facies | bulk sample | - | - | - |
| Archaeomagnetism | MIR107 | | Ci5-4 | Grey ash facies | bulk sample | - | - | - |
| Archaeomagnetism | MIR107 | | Ci5-5 | Grey ash facies | bulk sample | - | - | - |
| Archaeomagnetism | MIR107 | | Ci5-7 | Ash facies | bulk sample | - | - | - |
| Archaeomagnetism | MIR107 | | Ci5-11 | Carbonaceous facies | bulk sample | - | - | - |
| Archaeomagnetism | MIR107 | | Ci7-3 | Grey ash facies | bulk sample | - | - | - |
| Archaeomagnetism | MIR107 | | Ci7-6 | Grey ash facies | bulk sample | - | - | - |
| Archaeomagnetism | MIR107 | | Ci7-9 | Ash facies | bulk sample | - | - | - |
| Archaeomagnetism | MIR107 | | Ci7-10 | Grey ash facies | bulk sample | - | - | - |
| Archaeomagnetism | MIR107 | | Ci7-12 | Grey ash facies | bulk sample | - | - | - |
| Pollen, NPP | MIR4 | P20 | 34 | a | bulk sample | 80 | 15 | 1179 |
| Pollen, NPP | MIR4 | P22 | | a | bulk sample | 30 | 45 | 1195 |
| Pollen, NPP | MIR4 | Q22 | | a | bulk sample | 5 | 5 | 1198 |
| Pollen, NPP | MIR4 | P20 | 33 | b | bulk sample | 80 | 15 | 1176 |
| Pollen, NPP | MIR4 | P22 | | b | bulk sample | 35 | 40 | 1182 |
| Pollen, NPP | MIR4 | Q22 | | b | bulk sample | 5 | 5 | 1193 |
| Pollen, NPP | MIR4 | P22 | | g | bulk sample | 35 | 40 | 1192 |
| Pollen, NPP | MIR4 | Q21 | 192 | g | bulk sample | 79 | 50 | 1245 |
| Pollen, NPP | MIR4 | P20 | 180 | g | bulk sample | 16 | 37 | 1250 |
| Pollen, NPP | MIR4 | Q21 | | m | bulk sample | | | 1210 |
| Pollen, NPP | MIR4 | P20 | 166 | m | bulk sample | 41 | 78 | 1243 |
| Pollen, NPP | MIR4 | Q22 | 180 | m | bulk sample | 20 | 34 | 1250 |

# CHAPTER 6: SUPPLEMENTARY MATERIAL

## The *fumier* sequences of El Mirador: an approach to fire as a sociocultural practice and taphonomic agent.

Burguet-Coca, A., del Valle, H., Expósito, I., Herrejón Lagunilla, A., Buitkute, E. Cabanes, D., Cáceres, I., Carrancho, A., Villalaín, J.J.

## Supplementary material 2 (SM 2): Methods

***Phytoliths:*** Phytoliths were extracted following the extraction method Katz et al. (2010) extraction method. Between 30 and 40 mg of dry sediment were weighed and transferred to 0.5 conical centrifuge tubes. Then, 50 µl of 6N HCl was added in order to dissolve carbonate minerals. After the reaction ceased, 450 µl of sodium polytungstate 2.4 g/ml density was added to the solution. The tubes were then sonicated ca.10 min and centrifuged 5 min at 5000 rpm. The supernatant was transferred to a new 0.5-ml centrifuge tube. Then, the samples was homogenized an aliquot of 50 µl was placed on a microscope slide and covered with a 24 × 24 coverslip. Phytolith quantification and identification was carried out using a petrographic microscope Olympus BX41. To reduce quantification and identification errors, we counted the number of phytoliths present in a total of 20 fields at × 200 (Katz et al. 2010) and we identified a minimum of 200 individual phytoliths at × 400 (Albert and Weiner 2001). Phytolith concentrations are provided in grams of acid insoluble fraction (AIF) to avoid the effects of sediment diagenesis (Schiegl et al. 1996). Phytolith morphological identification followed the standard literature (Twiss et al. 1969; Piperno 1988, 2006; Rapp and Mulholland 1992; Twiss 1992; Portillo et al. 2014) and modern plant reference collections (Albert et al. 2000, 2016; Albert

and Weiner 2001; Tsartsidou et al. 2007). We followed the terminology of the International Code for Phytolith Nomenclature (ICPN 2.0) (Neumann et al. 2019).

***Spherulites*:** Dung spherulites extraction, identification, and quantification follow the method developed by Gur-Arieh et al. (2013). Between 30 and 40 mg of sediment was sieved through a 150-µm sieve mesh and placed in a 0.5-ml conical centrifuge tube. Then, 500 µl of 2.4 g/ml sodium polytungstate was added and the sample was homogenized and sonicated for 10 min before placing an aliquot of 50 µl on a microscope slide. The counting process was performed selecting 15 random fields at × 400 using crossed-polarized light (XPL) for a better identification of dung spherulites (Canti 1999).

***FTIR (bulk samples):*** The mineral composition of the samples was identified using a Fourier Jasco FT/IR-600 PLUS spectrometer. Infrared spectra were abotained using the conventional Kbr pellets methods collected between 4000 and 400 cm−1 wavelength range at 4 cm−1 resolution (Weiner et al. 1993). The spectra were interpreted using the position of the main peaks and the standards from the Kimmel Center of Archaeological Sciences (Weiner 2010). Thermally altered clay was identified on the basis of specific absorption picks in the clay spectrum (Berna et al. 2007). The origin of calcite Presence of anthropogenic or geogenic calcite was determined following Poduska et al. (2011) and Regev et al. (2010). The temperature determined for the bulk sediments has been obtained by crossing the data of the analysis of the altered clay with the presence/absence of high disordered calcite (HDC) in the spectra's.

***Bone diagenesis:*** Bone surface were analyzed with Stereomicroscope Euromex between 20x and 60x under a strong light (60 W). After, the

preparation of bone samples for ATR-FTIR measurements was doing by removing external surface areas with a micro-drill and a rotatory tool equipped with an abrasive diamond disc. Finally, each sample was hand-ground in an agate mortar in order to homogenize its size. We have attended to several diagenetic parameters that allow us screening the preservation stage.

The crystallinity of bone samples were measured through Splitting factor of the phosphate band at 567 $cm^{-1}$ and 605 $cm^{-1}$ (IRSF). Usually around 2.8-3.3 for modern bone and above 4.0 for extremely degraded bone (Weiner and Bar-Yosef 1990; Smith et al. 2007). Half-maximun of the $_{V3}$PO4 at 1035 $cm^{-1}$ (FWHM) was used in order to preview the bioapatite crystal size, decreasing from ~115 in modern bones to around 60 in degraded bone (Ellingham et al. 2016; Kimura-Suda and Ito 2017).

Regarding carbonates we have used Carbonates to phosphate ratio ($CO_3/PO_4$) and calcite to phosphate ratio ($Cal/PO_4$) in order to understand secondary calcite precipited. $CO_3/PO_4$ is calculated by dividing bands at 1415 $cm^{-1}$ and 1015 $cm^{-1}$. This ratio is related to the carbonate content of carbonate bioapatite. It is estimated around 0.31 in modern bone decreasing to ~0.15 in heavily degraded mineral. Additional carbonate from soils could increase the ratio above modern values (Wright and Schwarcz 1996). $Cal/PO_4$ used to show the amount of secondary calcite precipitated during diagenesis ($Cal/PO_4$). It is calculated by dividing the band intensity at 712 $cm^{-1}$ $_{v4}(CO_3)$ characteristic for calcite by the band intensity at 1015 $cm^{-1}$of phosphate. Similarly, the $CO_3/PO_4$ correction ($CO_3/PO_4$-corr) has been applied in cases where we have detected secondary calcite (Dal Sasso et al. 2016)

Taking into account the organic phase from archaeological bone remains we have attended to collagen content through ATR-FTIR. Amide I/$PO_4$ calculated by dividing the peak intensity of the Amide I band at 1660 $cm^{-1}$ by the peak intensity of the phosphate band at 1035 $cm^{-1}$. This parameter was determined in order to check the collagen degradation, following proposal in Lebon et al. (2016).

Finally attending to the need to understand the use of fire in a fumier context we have used FTIR parameters and bone coloration (Shipman et al. 1984; Nicholson 1993; Stiner et al. 1995; Surovell and Stiner 2001; Cáceres 2002; Lebon et al. 2010; Pérez et al. 2017) related to heating and burning. For this issue, we have used the indexes presented in Thompson et al. (2013) and Ellingham et al. (2016): IRSF; $CO_3/PO_4$; PHT; amide I/$PO_4$; amide I/$CO_3$; 900/1035 $cm^{-1}$; FWHM; $CO_3/CO_3$.

The baseline used to calculate band and area intensities was defined by two points for each parameter. The phosphate $_{v3}PO_4$ band was measured between values from 1160 to 890 $cm^{-1}$. The Amide I band area was measured between values from 1710 to 1590 $cm^{-1}$. For $_{V3}CO_3$ band at 1415 $cm^{-1}$ a baseline between values from 1590 to 1290 $cm^{-1}$ was applied and for $_{v4}CO_3$ between values from 730 and 700 $cm^{-1}$. Finally, $_{v4}PO_4$ was measured between 495 and 750 $cm^{-1}$.

FTIR bone analysis was performed in ATR mode (Beasley et al. 2014). Spectra were collected on a Vertex 70 spectrometer (Bruker) from MNHN (Paris) with a resolution of 2 $cm^{-1}$ and 64 scans in the range 4000-370 $cm^{-1}$. Around 1 mg of sample powder was pressed on the surface of a diamond crystal. In order to determine homogeneity to statistically compare, anvil pressure on the ATR

crystal was adjusted from 0.5 N.m-2 to obtain a raw absorbance of 0.5 for the $_{v3}PO_4$ band around 1015 $cm^{-1}$ (Lebon et al. 2016). Spectra analysis was performed using Omnic 9.8 software (Thermo Scientific).

***Paleoparasitologist:*** Samples for Paleoparasitological testing were taken during the 2019 field campaign, in total, collecting 20 samples in various sizes from 45 gr to 210 gr. Following our proposed sampling strategy, samples were collected from the fumiers layers formations avoiding the areas that might have been mostly affected by the intense heat and pinpointing the potentially unburned formation parts. In total, we received 2271 gr of sediment, represented as 20 samples.

For samples processing, we used the same methodology for each sample independently and tested the samples together with the Paleoparasitogists team in Besancon, France. The used protocol consists of three major steps such as rehydration, homogenization and micro-sieving (RHM). The RHM protocol does not involve flotation techniques and micro-sieving is used instead. This adjustment allows recovering all types of parasite eggs with no selection. The RHM protocol may be time-consuming but allows the detection of higher parasite diversity in comparison to other protocols where some parasites species eggs damaging acids and sodium hydroxide are being used (Dufour and Le Bailly 2013).

To perform samples preparation, we used 5 gr of the original sample and followed RHM extraction protocol. First, 5 gr of the sample (sediment) were weighted and isolated from the original and remaining sample content. Second, the isolated 5 gr of the sediment were rehydrated for 7 days in a solution composed of 50ml 0,5% trisodium phosphate, 50ml 5% glycerinated solution

and several drops of 10% formalin solution. After 7 days of rehydration, we performed homogenization where we crushed the sample in a mortar and submitted it to ultra-sounds (50–60 Hz) for 1 min. Then the crushed and treated sample was strained through 315 μm, 160 μm, 50 μm, and 25 μm meshes under a constant flux of ultrapure water. Finally, the two screenings (50 μm and 25 μm) were transferred into 4 ml polyvinyl chloride (PVC) tubes, named after fraction 50 and fraction 25.

For the microscopic analysis, we used a light microscope (Leica DM-2000 LED) coupled with a digital camera (Leica ICC50-HD) and analysed either 4 or 6 slides per fraction from fraction 50 μm and 25 μm independently.

***Rock magnetic:*** Hereunder, the Rock magnetic laboratory procedures are briefly summarized. All the analyses were carried out at the Paleomagnetic Laboratory of the University of Burgos.

**a. Thermomagnetic curves (magnetization vs. temperature)**

Thermomagnetic curves consist of the measurement of the induced magnetization under the application of a constant field (in this case, ~38 mT) while temperature is increased/decreased, respectively. This experiment allow to infer the main ferromagnetic minerals present in the samples (through the determination of the Curie temperature/s), as well as to assess the temperatures reached by means of the reversibility degree (coincidence of the heating/cooling curves) (i.e. Hrouda et al. 2003; Carrancho et al. 2016). Mineralogical transformations during the experiment (resulting in irreversible thermomagnetic curves) suggest that the sample had reached temperatures lower than the maximum one applied.

Thermomagnetic curves up to 700 ºC (on air) were carried out on bulk (unoriented) samples from representative facies. The experiments were performed with a Magnetic Measurements' Variable Field Traslation Balance.

**b. Anisotropy of Magnetic Susceptibility (AMS)**

Anisotropy of Magnetic Susceptibility (AMS) is used to know the magnetic fabric of the materials. This parameter is useful to assess possible mechanical alterations (i.e.: water flows) through the orientations of the axes of the magnetic ellipsoid obtained from the tensor of magnetic susceptibility.

56 oriented specimens (volumen of each specimen: ~3.6 $cm^3$) of ash and carbonaceous facies were used to analyse the AMS. It was measured with a Kappabridge KLY-4S (AGICO), using the automated rotator system.

**c. Hysteresis loops**

This experiment illustrates the variation of the induced magnetization according to the applied field and is useful to assess the domain state, the granulometry and the contribution of ferro-, dia- and paramagnetic minerals. Hysteresis loops up to ±1 T were performed with a Magnetic Measurements' Variable Field Traslation Balance.

**Palynology:**

The palynological samples analysed were collected from the different facies that are described for MIR4 level simultaneously to the archaeological work. We study three samples from four sedimentary facies (a, b, g and m).

The samples are treated with HCl, NaOH, HF, and flotation with Thoulet's solution (Goeury and de Beaulieu 1979; Burjachs et al. 2003). Fossil pollen,

spores and NPP were identified using published keys (Van Geel 1978; Jarzen and Elsik 1986; van Geel 1986; Moore et al. 1991; Reille 1992, 1995; Miola 2012) and a modern pollen reference collection. The samples were analysed with an Olympus Cx41 microscope at 600 magnifications.

AP/ NAP percentages have been calculated excluding Asteraceae and Cerealia-type from the basic sum since they have a specific pollination system and/or are favoured by anthropic activity. The minimum statistically meaningful values of NPPs were stablished until maximum pollen counts had been reached (minimum of 100-150 pollens counted). We have excluded from the NPPs basic sum the types with an indeterminate ecological origin (Pseudoschizaea, type 303 and protists). For the Palynological Concentration (PC) we have used the volumetric method proposed for Loublier (1978).

We have categorized the post-depositional damage observed in pollen grains into three types: thermoalteration, fragmentation and compaction and we have calculated the percentages of the alterations with respect to the total pollen identified.

Albert RM, Ruíz JA, Sans A (2016) PhytCore ODB: A new tool to improve efficiency in the management and exchange of information on phytoliths. Journal of Archaeological Science 68:98–105. https://doi.org/10.1016/j.jas.2015.10.014

Albert R-M, Weiner L, Bar-Yosef O, Meignen L (2000) Phytoliths in the Middle Palaeolithic Deposits of Kebara Cave, Mt Carmel, Israel: Study of the Plant Materials used for Fuel and Other Purposes. Journal of Archaeological Science 27:931–947

Albert RM, Weiner S (2001) Study of phytoliths in prehistoric ash layers from Kebara and Tabun Caves using a quantitative approach. In: Meunier JD, Colin F (eds) Phytoliths: application in Earth Sciences and Human History. A. A. Balkema Publishers, Lisse, pp 251–266

Beasley MM, Bartelink EJ, Taylor L, Miller RM (2014) Comparison of transmission FTIR, ATR, and DRIFT spectra: implications for

assessment of bone bioapatite diagenesis. Journal of Archaeological Science 46:16–22. https://doi.org/10.1016/j.jas.2014.03.008

Berna F, Behar A, Shahack-Gross R, et al (2007) Sediments exposed to high temperatures: reconstructing pyrotechnological processes in Late Bronze and Iron Age Strata at Tel Dor (Israel). Journal of Archaeological Science 34:358–373

Burjachs F, López-Sáez JA, Iriarte-Chiapusso MJ (2003) Metodología arqueopalinológica. In: Buxó R, Piqué R (eds) La recogida de muestras en arqueobotànica: objetivos y propuestas metodológicas. Museu d'Arqueologia de Catalunya, Barcelona, pp 9–16

Cáceres I (2002) Tafonomía de yacimientos antrópicos en karst. Complejo Galería (Sierra de Atapuerca, Burgos), Vanguard Cave (Gibraltar) y Abric Romaní (Capellades, Barcelona). Universitat Rovira i Virgili

Canti MG (1999) The Production and Preservation of Faecal Spherulites: Animals, Environment and Taphonomy. Journal of Archaeological Science 26:251–258. http://dx.doi.org/10.1006/jasc.1998.0322

Carrancho Á, Herrejón Lagunilla Á, Vergès JM (2016) Three archaeomagnetic applications of archaeological interest to the study of burnt anthropogenic cave sediments. Quaternary International 414:244–257. https://doi.org/10.1016/J.QUAINT.2015.10.010

Dal Sasso G, Lebon M, Angelini I, et al (2016) Bone diagenesis variability among multiple burial phases at Al Khiday (Sudan) investigated by ATR-FTIR spectroscopy. Palaeogeography, Palaeoclimatology, Palaeoecology 463:168–179. https://doi.org/10.1016/j.palaeo.2016.10.005

Dufour B, Le Bailly M (2013) Testing new parasite egg extraction methods in paleoparasitology and an attempt at quantification. International Journal of Paleopathology 3:199–203. https://doi.org/10.1016/j.ijpp.2013.03.008

Ellingham STD, Thompson TJU, Islam M (2016) The Effect of Soft Tissue on Temperature Estimation from Burnt Bone Using Fourier Transform Infrared Spectroscopy. J Forensic Sci 61:153–159. https://doi.org/10.1111/1556-4029.12855

Goeury C, de Beaulieu JL (1979) À propos de la concentration du pollen à l'aide de la liqueur de Thoulet dans les sédiments minéraux. Pollen et Spores XXI:239–251

Gur-Arieh S, Mintz E, Boaretto E, Shahack-Gross R (2013) An ethnoarchaeological study of cooking installations in rural Uzbekistan: Development of a new method for identification of fuel sources. Journal of Archaeological Science. https://doi.org/10.1016/j.jas.2013.06.001

Hrouda F, Müller P, Hanák J (2003) Repeated progressive heating in susceptibility vs. temperature investigation; a new palaeotemperature indicator? Physics and Chemistry of the Earth 28:653–657

Jarzen DM, Elsik WC (1986) Fungal palynomorphs recovered from recent river deposits, Luangwa valley, Zambia. Palynology 10:35–60

Katz O, Cabanes D, Weiner S, et al (2010) Rapid phytolith extraction for analysis of phytolith concentrations and assemblages during an excavation: an application at Tell es-Safi/Gath, Israel. Journal of Archaeological Science 37:1557–1563. https://doi.org/10.1016/j.jas.2010.01.016

Kimura-Suda H, Ito T (2017) Bone quality characteristics obtained by Fourier transform infrared and Raman spectroscopic imaging. Journal of Oral Biosciences 59:142–145. https://doi.org/10.1016/j.job.2017.04.002

Lebon M, Reiche I, Bahain J-J, et al (2010) New parameters for the characterization of diagenetic alterations and heat-induced changes of fossil bone mineral using Fourier transform infrared spectrometry. Journal of Archaeological Science 37:2265–2276. https://doi.org/10.1016/j.jas.2010.03.024

Lebon M, Reiche I, Gallet X, et al (2016) Rapid Quantification of Bone Collagen Content by ATR-FTIR Spectroscopy. Radiocarbon 58:131–145. https://doi.org/10.1017/RDC.2015.11

Loublier Y (1978) Application de l'analyse pollinique à l'étude du paléoenvironnement du remplissage Würmien de la grotte de L'Arbreda (Espagne). PhD Thesis, Académie de Montpellier (U.S.T.L.)

Miola A (2012) Tools for non-pollen palynomorphs (NPPs) analysis: A list of Quaternary NPP types and reference literature in english language (1972-2011). Review of Palaeobotany and Palynology 186:142–161. https://doi.org/10.1016/j.revpalbo.2012.06.010

Moore PD, Webb JA, Collinson ME (1991) Pollen Analysis, 2a edn. Blackwell Scientific Publications, Oxford

Neumann K, Strömberg CAE, Ball T, et al (2019) International Code for Phytolith Nomenclature (ICPN) 2.0. Annals of Botany 124:189–199. https://doi.org/10.1093/aob/mcz064

Nicholson RA (1993) A Morphological Investigation of Burnt Animal Bone and an Evaluation of its Utility in Archaeology. Journal of Archaeological Science 20:411–428. https://doi.org/10.1006/jasc.1993.1025

Pérez L, Sanchis A, Hernández CM, et al (2017) Hearths and bones: An experimental study to explore temporality in archaeological contexts based on taphonomical changes in burnt bones. Journal of Archaeological Science: Reports 11:287–309. http://dx.doi.org/10.1016/j.jasrep.2016.11.036

Piperno DR (1988) Phytolith Analysis. An Archaeological and Geological Perspective. Academic Press, San Diego

Piperno DR (2006) Phytoliths: A comprehensive guide for archaeologists and paleoecologists. AltaMira Press, Lanham

Poduska KM, Regev L, Boaretto E, et al (2011) Decoupling Local Disorder and Optical Effects in Infrared Spectra: Differentiating Between Calcites with Different Origins. Advanced Materials 23:550–554. https://doi.org/10.1002/adma.201003890

Portillo M, Kadowaki S, Nishiaki Y, Albert RM (2014) Early Neolithic household behavior at Tell Seker al-Aheimar (Upper Khabur, Syria): a comparison to ethnoarchaeological study of phytoliths and dung spherulites. Journal of Archaeological Science 42:107–118. http://dx.doi.org/10.1016/j.jas.2013.10.038

Rapp G, Mulholland SC (1992) Phytolith Systematics. Emerging Issues. Plenum Press, New York

Regev L, Poduska KM, Addadi L, et al (2010) Distinguishing between calcites formed by different mechanisms using infrared spectrometry: archaeological applications. Journal of Archaeological Science 37:3022–3029

Reille M (1992) Pollen et Spores d'Europe et d'Afrique du nord. Laboratoire de Botanique Historique et Palynologie, Marseille

Reille M (1995) Pollen et Spores d'Europe et d'Afrique du Nord (Supplément 1). Laboratoire de Botanique Historique et Palynologie, CNRS, Marseille

Schiegl S, Goldberg P, Bar-Yosef O, Weiner S (1996) Ash deposits in Hayonim and Kebara Caves, Israel: Macroscopic, microscopic and mineralogical observations, and their archaeological implications. Journal of Archaeological Science 23:763–781. https://doi.org/10.1006/jasc.1996.0071

Shipman P, Foster G, Schoeninger M (1984) Burnt bones and teeth: an experimental study of color, morphology, crystal structure and shrinkage. Journal of Archaeological Science 11:307–325. https://doi.org/10.1016/0305-4403(84)90013-X

Smith CI, Nielsen-Marsh CM, Jans MME, Collins MJ (2007) Bone diagenesis in the European Holocene I: patterns and mechanisms. Journal of Archaeological Science 34:1485–1493. https://doi.org/10.1016/j.jas.2006.11.006

Stiner MC, Kuhn SL, Weiner S, Bar-Yosef O (1995) Differential Burning, Recrystallization, and Fragmentation of Archaeological Bone. Journal of Archaeological Science 22:223–237. https://doi.org/10.1006/jasc.1995.0024

Surovell TA, Stiner MC (2001) Standardizing Infra-red Measures of Bone Mineral Crystallinity: an Experimental Approach. Journal of Archaeological Science 28:633–642. https://doi.org/10.1006/jasc.2000.0633

Thompson TJU, Islam M, Bonniere M (2013) A new statistical approach for determining the crystallinity of heat-altered bone mineral from FTIR spectra. Journal of Archaeological Science 40:416–422. https://doi.org/10.1016/j.jas.2012.07.008

Tsartsidou G, Lev-Yadun S, Albert R-MR-M, et al (2007) The phytolith archaeological record: strengths and weaknesses evaluated based on a quantitative modern reference collection from Greece. Journal of Archaeological Science 34:1262–1275. https://doi.org/10.1016/j.jas.2006.10.017

Twiss PC (1992) Predicted World Distribution of C3 and C4 grass phytoliths. In: Rapp JrG, Mulholland SC (eds) Phytolith systematics. Emerging issues. Plenum Press, London/New York, pp 113–128

Twiss PC, Suess E, Smith RM (1969) Morphological classification of grass phytoliths. Soil Science Society of America Proceedings 33:109–115

van Geel B (1986) Application of fungal and algal remains and other microfossils in palynological analyses. In: Berglund B (ed) Handbook of Holocene Palaeoecology and Palaeohydrology. John Wiley & Sons Ltd, Chichester

Van Geel B (1978) A palaeoecological study of Holocene peat bog sections in Germany and the Netherlands, based on the analysis of pollen, spores and macro-and microscopic remains of fungi, algae, cormophytes and animals. Review of palaeobotany and palynology 25:1–120

Weiner L, Bar-Yosef O (1990) States of Preservation of Bones from Prehistoric Sites in the Near East: A Survey. Journal of Archaeological Science 17:187–196

Weiner S (2010) Microarchaeology. Beyond the Visible Archaeological Record. Cambridge University Press, New York

Weiner S, Golberg P, Bar-Yosef O (1993) Bone Preservation in Kebara Cave, Israel using On-Site Fourier Transform Infrared Spectrometry. Journal of Archaeological Science 20:613–627

Wright LE, Schwarcz HP (1996) Infrared and Isotopic Evidence for Diagenesis of Bone Apatite at Dos Pilas, Guatemala: Palaeodietary Implications. Journal of Archaeological Science 23:933–944. https://doi.org/10.1006/jasc.1996.0087

**CHAPTER 6: SUPPLEMENTARY MATERIAL**

**The fumier sequences of El Mirador: an approach to fire as a sociocultural practice and taphonomic agent.**

Burguet-Coca, A., del Valle, H., Expósito, I., Herrejón Lagunilla, A., Buitkute, E. Cabanes, D., Cáceres, I., Carrancho, A., Villalaín, J.J.

**Supplementary material 3 (SM 3):** Main diagenetic parameters through ATR-FTIR and thermal alterations

**Legend:** Bones organic parameters (Am/P; AmIII/P; Am/$C_1$; Am/$C_2$; N wt%; Collagen wt%); Bones inorganic parameters (CI or IRSF; C/P; BPI; API; C/C;$CO_3$/P;FWHM;PHT); Secondary calcite in bone structure (Cal/P). Correlation of the amount of collagen obtained by the extraction protocol and by ATR-FTIR through the Am/P index. The data set is found in (Del Valle et al., JAS)

| | **Facies *a* MIR 105** Middle Bronze Age | | **Facies *v* MIR 205** 5748-5610 cal yr B.P. | | **Facies *v* MIR 108** 6447-6310 cal yr B.P. | | **Facies tf MIR 107** 6491-6390 cal yr B.P. | | **Facies r(m)MIR 107** 6491-6390 cal yr B.P. | |
|---|---|---|---|---|---|---|---|---|---|---|
| | **mean** | **SD** | **mean** | **SD** | **mean** | **SD** | **mean** | **SD** | **mean** | **SD** |
| **Am/P** | 0.076 | 0.050 | 0.075 | 0.047 | 0.081 | 0.046 | 0.005 | 0.002 | 0.000 | 0.000 |
| **CI** | 3.593 | 0.547 | 3.438 | 0.082 | 3.464 | 0.098 | 4.061 | 0.294 | 5.394 | 0.388 |
| **C/P** | 0.297 | 0.079 | 0.322 | 0.056 | 0.305 | 0.035 | 0.191 | 0.023 | 0.127 | 0.022 |
| **BPI** | 0.635 | 0.205 | 0.686 | 0.156 | 0.644 | 0.136 | 0.375 | 0.070 | 0.206 | 0.035 |
| **API** | 0.138 | 0.055 | 0.278 | 0.101 | 0.309 | 0.145 | 0.080 | 0.018 | 0.032 | 0.006 |
| **C/C** | 0.850 | 0.097 | 0.786 | 0.032 | 0.792 | 0.025 | 0.788 | 0.078 | 0.914 | 0.052 |
| **Cal/P** | 0.001 | 0.002 | 0.000 | 0.000 | 0.000 | 0.000 | 0.000 | 0.000 | 0.011 | 0.006 |
| **$CO_3$/P** | 0.139 | 0.062 | 0.153 | 0.030 | 0.143 | 0.021 | 0.123 | 0.014 | 0.116 | 0.033 |
| **Am/$C_1$** | 0.366 | 0.203 | 0.445 | 0.214 | 0.404 | 0.189 | 0.101 | 0.063 | 0.000 | 0.000 |
| **PHT** | 0.000 | 0.000 | 0.000 | 0.000 | 0.000 | 0.000 | 0.047 | 0.081 | 0.353 | 0.034 |
| **AmIII/P** | 0.016 | 0.009 | 0.012 | 0.009 | 0.014 | 0.011 | 0.000 | 0.000 | 0.000 | 0.000 |
| **Am/$C_2$** | 0.821 | 0.516 | 0.970 | 0.485 | 0.913 | 0.468 | 0.155 | 0.101 | 0.000 | 0.000 |
| **FWHM** | 81.142 | 8.560 | 86.333 | 7.949 | 82.360 | 5.777 | 70.474 | 3.790 | 67.138 | 5.019 |

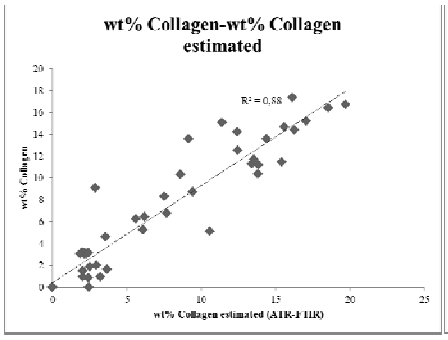


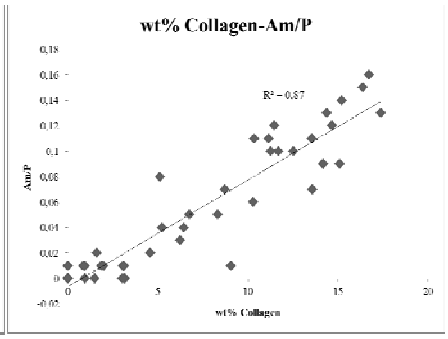

| Sample | facies | Burnt Stage |
|---|---|---|
| **MIR105/T12/153** | a | 2 |
| **MIR105/T12/78** | a | 1 |
| **MIR105/T13/103** | a | 2-3 |
| **MIR105/T12/147** | a | Boiled |
| **MIR105/T13/122** | a | 1 |
| **MIR105/T12/129** | a | 2 |
| **MIR105/T12/174** | a | 1 |
| **MIR105/T12/176** | a | 5 |
| **MIR105/T12/171** | a | 2 |
| **MIR105/T12/76** | a | 2-3 |
| **MIR205/Q38/53** | v 200 | Boiled |
| **MIR205/Q37/26** | v 200 | 2-3 |
| **MIR205/P36/18** | v 200 | Boiled |
| **MIR205/P36/20** | v 200 | Boiled |
| **MIR205/O38/28** | v 200 | 2 |
| **MIR205/O38/36** | v 200 | Boiled |
| **MIR205/P38/25** | v 200 | 3 |
| **MIR205/Q37/35** | v 200 | 2 |
| **MIR205/O37/6** | v 200 | Boiled |
| **MIR205/O37/9** | v 200 | Boiled |
| **MIR108/V13/49** | v 100 | Boiled |
| **MIR108/V12/12** | v 100 | 2-3 |
| **MIR108/V12/17** | v 100 | 1 |
| **MIR108/V12/5** | v 100 | Not Burned |
| **MIR108/V12/21** | v 100 | 2-3 |
| **MIR108/V12/19** | v 100 | Boiled |
| **MIR108/V12/15** | v 100 | Not Burned |
| **MIR108/W13/93** | v 100 | 2 |
| **MIR108/V12/60** | v 100 | Boiled |
| **MIR108/V12/23** | v 100 | 2 |
| **MIR107/V13/214** | tf | 2-3 |
| **MIR107/V13/198** | tf | 2-3 |
| **MIR107/V13/200** | tf | 2-3 |
| **MIR107/V13/196** | tf | 2-3 |
| **MIR107/V13/211** | tf | 4 |
| **MIR107/V13/217** | tf | 2 |
| **MIR107/V13/203** | tf | 2-3 |
| **MIR107/V13/194** | tf | 2-3 |
| **MIR107/V13/227** | tf | 2 |
| **MIR107/V13/225** | tf | 4 |
| **MIR107/V13/115** | r(m) | 5 |
| **MIR107/V13/104** | r(m) | 5 |
| **MIR107/V13/92** | r(m) | 5 |
| **MIR107/V13/113** | r(m) | 5 |
| **MIR107/V13/97** | r(m) | 5 |
| **MIR107/V13/93** | r(m) | 5 |
| **MIR107/V13/103** | r(m) | 5 |

**CHAPTER 6: SUPPLEMENTARY MATERIAL**

**The fumier sequences of El Mirador: an approach to fire as a sociocultural practice and taphonomic agent.**

Burguet-Coca, A., del Valle, H., Expósito, I., Herrejón Lagunilla, A., Buitkute, E. Cabanes, D., Cáceres, I., Carrancho, A., Villalaín, J.J.

**Supplementary material 4 (SM 4): FTIR resultrs from bulk samples**

**Legend:** Ca=Calcite; Cl=Clay; Qz=Quartz; Dah=Dahllite (carbonated hydroxylapatite); b=thermally altered clay; nb= not thermally altered clay; HDC=High disorder calcite.

| Level | Square | Num. | facie | Episode | Main Mineral | Clay | Temperature range from clay | Calcite origin | HDC |
|---|---|---|---|---|---|---|---|---|---|
| MIR105 | S15 | 108 | a | - | Cl, Ca, Qz, Dah | b | 500-400 | Ash | |
| MIR105 | S15 | 107 | a | - | Cl, Ca, Qz, Dah | b | 800-700 | Ash | |
| MIR105 | S15 | 106 | a | - | Cl, Ca, Qz, Dah | b | 500-400 | Ash | |
| MIR105 | S15 | 105 | a | - | Cl, Ca, Qz, Dah | b | 500-400 | Ash | HDC? |
| MIR105 | S15 | 104 | a | - | Cl, Ca, Qz, Dah | b | 500-400 | Ash | HDC |
| MIR105 | S15 | 103 | a | - | Cl, Ca, Qz, Dah | b | 500-400 | Ash | |
| MIR105 | S15 | 102 | a | - | Cl, Ca, Qz, Dah | b | 500-400 | Ash | |
| MIR105 | S15 | 101 | a | - | Cl, Ca, Qz, Dah | b | > 600 ºC | Ash | HDC |
| MIR105 | S15 | 100 | a | - | Cl, Ca, Qz, Dah | b | > 600 ºC | Ash | HDC |
| MIR105 | T12 | 79 | a | | Cl=Op, Ca,Dah | b | >400 ºC | Ash | |
| MIR105 | T12 | 130 | a | | Cl, Ca, Dah | b? | unburnt | Ash | |
| MIR105 | T12 | 148 | a | | Cl, Op?, Ca, Dah | nb | unburnt | Ash | |
| MIR105 | T12 | 154 | a | | Cl, Op, Ca, Dah | b | <500 ºC | Ash | |
| MIR105 | T12 | 172 | a | | Cl, Op?, Ca, Dah | b | <600 ºC | Ash | |
| MIR105 | T12 | 177 | a | | Cl=Ca, Op?, Dah | b | >500 ºC | Ash | |
| MIR105 | T13 | 104 | a | | Op, Cl, Ca, Dah | nb | unburnt | Ash | |
| MIR105 | T13 | 121 | a | | Op, Cl, Ca, Dah | b | >500 ºC | Ash | |
| MIR105 | T12 | 77 | a | | Cl=Op, Ca, Dah | b | >500 ºC | Ash | |
| MIR105 | T12 | 175 | a | | Cl, Op, Ca, Dah | b | <500 ºC | Ash | |
| MIR105 | V12 | 5 | a | | Cl, Op, Ca, Dah | nb | unburnt | Ash | |
| MIR104 | T15 | 188 | b | 1 | Ca, Cl, Qz, Dah | b | 800-700 | Ash | HDC |
| MIR104 | T15 | 187 | b | 1 | Ca=Cl, Qz, Dah | b | 500-400 | Ash | |
| MIR104 | T15 | 185 | b | 2 | Cl=Ca, Qz, Dah | b | 400 | Ash | HDC |
| MIR104 | S15 | 104 | b | 2 | Ca, Cl, Qz, Dah | b | 500-400 | Ash | HDC |
| MIR104 | T15 | 186 | c | 1 | Ca=Cl, Qz, Dah | b | 400-300 | Ash | HDC |
| MIR104 | S15 | 103 | c | 2 | Cl, Ca, Qz, Dah | b | 500-400 | Ash | |
| MIR107 | V13 | 98 | r(m) | | Ca, Cl, Op?, Dah | b | 700-800 ºC | Ash | |
| MIR107 | V13 | 99 | r(m) | | Ca, Cl, Op?, Dah | b | 700-800 ºC | Ash | |
| MIR107 | V13 | 114 | r(m) | | Ca, Cl, Op?, Dah | b | 700-800 ºC | Ash | HDC |
| MIR107 | V13 | 116 | r(m) | | Ca, Cl, Op?, Dah | b | 700-800 ºC | Ash | HDC |
| MIR107 | V13 | 105 | r(m) | | Ca, Cl, Op?, Dah | b | 700-800 ºC | Ash | |
| MIR107 | v13 | 209 | r(m) | | Ca, Cl, Op, Dah | b | 700-800 ºC | Ash | HDC |
| MIR107 | V13 | 195 | tf | | Cl,Op?, Ca, Dah | b | <600 ºC | Ash | |
| MIR107 | V13 | 197 | tf | | Ca=Cl, Op, Dah | b | <600 ºC | Ash | |
| MIR107 | V13 | 201 | tf | | Ca,Cl,Op?,Dah | b | <600 ºC | Ash | |
| MIR107 | V13 | 202 | tf | | Cl, Ca, Op?, Dah | b | <600 ºC | Ash | |
| MIR107 | V13 | 204 | tf | | Ca, Cl, Dah | b | <600 ºC | Ash | |
| MIR107 | V13 | 212 | tf | | Cl, Op, Ca, Dah | b | <600 ºC | Ash | |
| MIR107 | V13 | 215 | tf | | Cl, Ca, Dah | b | <600 ºC | Ash | |
| MIR107 | V13 | 218 | tf | | Cl, Op, Ca, Dah | b | <600 ºC | Ash | |
| MIR107 | V13 | 226 | tf | | Cl, Op, Ca, Dah | b | 700-800 ºC | Ash | HDC |
| MIR107 | V13 | 228 | tf | | Cl, Op?, Ca, Dah | b | >700 ºC | Ash | |
| MIR107 | V13 | 208 | tf | | Cl, Op?, Ca, Dah | b | 700 ºC | Ash | HDC |
| MIR108 | V12 | 18 | v | | Cl, Op?, Ca, Dah | nb | unburnt | Ash | |
| MIR108 | V12 | 20 | v | | Cl, Op, Ca, Dah | nb | unburnt | geogenic calcite | |
| MIR108 | V12 | 6 | v | | Op, Cl, Ca, Dah | nb | unburnt | geogenic calcite | |
| MIR108 | V12 | 13 | v | | Cl, Op, Ca, Dah | nb | unburnt | Ash | |
| MIR108 | V12 | 16 | v | | Cl, Op?, Ca, Dah | nb | unburnt | Ash | |
| MIR108 | V12 | 22 | v | | Cl, Op?, Ca, Dah | nb | unburnt | geogenic calcite | |
| MIR108 | V12 | 24 | v | | Cl, Op?, Ca, Dah | nb | unburnt | geogenic calcite | |
| MIR108 | V12 | 61 | v | | Cl, Op, Ca, Dah | nb | unburnt | geogenic calcite | |
| MIR108 | V13 | 50 | v | | Cl, Ca, Dah, Qz | nb | unburnt | geogenic calcite | |
| MIR108 | V13 | 94 | v | | Cl, Op, Ca, Dah | nb | unburnt | geogenic calcite | |
| MIR108 | V13 | 64 | v | | Cl, Op, Ca, Dah | nb | unburnt | geogenic calcite | |
| MIR205 | O37 | 7 | v | | Cl=Op, Ca, Dah | b? | <400 ºC | Ash | |
| MIR205 | O37 | 10 | v | | Cl, Op, Ca, Dah | b? | <400 ºC | Ash | HDC |
| MIR205 | O38 | 37 | v | | Cl, Op?, Ca, Dah | nb | unburnt | geogenic calcite | |
| MIR205 | P36 | 19 | v | | Cl=Op, Ca, Dah | nb | unburnt | Ash | |
| MIR205 | P36 | 21 | v | | Cl, Op?, Ca, Dah | nb | unburnt | Ash | |
| MIR205 | P38 | 26 | v | | Cl, Op?, Ca, Dah | nb | unburnt | Ash | |
| MIR205 | Q37 | 27 | v | | Op=Cl, Ca, Dah | nb | unburnt | Ash | |
| MIR205 | Q37 | 36 | v | | Op, Cl, Ca, Dah | b | 400-500 ºC | Ash | |
| MIR205 | Q38 | 29 | v | | Op=Cl, Dah, Qz | nb | unburnt | - | |
| MIR205 | Q38 | 54 | v | | Op, Cl, Dah, Qz | nb | unburnt | - | |
| MIR205 | O37 | 14 | v | | Ca, Cl, Op, Dah | b | <500 ºC | Ash | |

**CHAPTER 6: SUPPLEMENTARY MATERIAL**

**The fumier sequences of El Mirador: an approach to fire as a sociocultural practice and taphonomic agent.**

Burguet-Coca, A., del Valle, H., Expósito, I., Herrejón Lagunilla, A., Buitkute, E. Cabanes, D., Cáceres, I., Carrancho, A., Villalaín, J.J.

**Supplementary material 5 (SM 5): Phytoliths and Dung Spherulites results**

| Sample | Square | Level | facie | hered morp | lted morpho | out anatomi | cass inflores | c %Grass leaf | otyledonous | Wood and B | Phyt x g/AIF | Spherulites x g/sediment |
|---|---|---|---|---|---|---|---|---|---|---|---|---|
| 188 | T15 | MIR104 | b | 23.55 | 18.15 | 19.31 | 3.47 | 28.96 | 0.00 | 6.56 | 70,558,332 | 53,708,453 |
| 187 | T15 | MIR104 | b | 3.29 | 0.41 | 56.38 | 4.94 | 29.63 | 0.00 | 5.35 | 227,166,093 | 727,969,024 |
| 186 | T15 | MIR104 | c | 3.03 | 0.00 | 37.66 | 7.79 | 36.36 | 0.00 | 15.15 | 146,747,702 | 215,393,276 |
| 185 | T15 | MIR104 | b | 2.25 | 0.00 | 53.18 | 8.24 | 29.21 | 0.00 | 7.12 | 718,872,638 | 1,620,213,819 |
| 104 | S15 | MIR104 | b | 6.69 | 0.79 | 49.21 | 4.72 | 33.46 | 0.00 | 4.72 | 134,961,503 | 1,425,388,519 |
| 103 | S15 | MIR104 | c | 1.61 | 0.00 | 50.40 | 5.65 | 34.68 | 0.00 | 7.66 | 397,293,418 | 290,218,484 |
| 108 | S15 | MIR105 | a | 12.93 | 0.76 | 50.19 | 7.98 | 21.67 | 0.00 | 6.08 | 731,398,732 | 737,819,877 |
| 107 | S15 | MIR105 | a | 7.09 | 0.79 | 54.33 | 6.69 | 27.56 | 0.00 | 3.54 | 998,183,201 | 468,678,834 |
| 106 | S15 | MIR105 | a | 7.09 | 0.37 | 55.22 | 7.09 | 25.75 | 0.00 | 4.48 | 213,079,790 | 587,255,458 |
| 105 | S15 | MIR105 | a | 6.40 | 0.00 | 52.40 | 10.00 | 26.00 | 0.00 | 5.20 | 212,073,329 | 496,113,693 |
| 104 | S15 | MIR105 | a | 1.16 | 0.39 | 51.16 | 11.63 | 31.01 | 0.00 | 4.65 | 190,226,055 | 510,406,979 |
| 103 | S15 | MIR105 | a | 9.34 | 0.39 | 51.36 | 7.39 | 26.85 | 0.00 | 4.67 | 197,555,407 | 455,342,445 |
| 102 | S15 | MIR105 | a | 4.28 | 1.17 | 43.19 | 9.34 | 33.07 | 0.00 | 8.95 | 121,390,393 | 754,104,156 |
| 101 | S15 | MIR105 | a | 6.41 | 2.14 | 50.89 | 4.98 | 29.89 | 0.00 | 5.69 | 977,534,533 | 1,136,459,196 |
| 100 | S15 | MIR105 | a | 3.93 | 0.36 | 52.14 | 7.86 | 29.64 | 0.36 | 5.36 | 1,782,567,907 | 670,958,956 |